AIMS Mathematics, 9(7): 18984–19014.
DOI: 10.3934/math.2024924
Received: 26 February 2024
Revised: 28 May 2024
Accepted: 29 May 2024
Published: 06 June 2024

http://www.aimspress.com/journal/Math

Research article

Exploring dynamic behavior and bifurcations in a Filippov neuronal system with a double-tangency singularity

Yi Yang[1,2,*], Rongfeng Li[3], Xiangguang Dai[1,2], Haiqing Li[1,2] and Changcheng Xiang[4,*]

[1] College of Computer Science and Engineering, Chongqing Three Gorges University, Chongqing, 404100, China
[2] Key Laboratory of Intelligent Information Processing and Control of Chongqing Municipal Institutions of Higher education, Chongqing Three Gorges University, Chongqing, 404100, China
[3] School of Intelligent Technology, Chongqing Preschool Education College, Chongqing, 404047, China
[4] School of Mathematics and Statistics, Hubei Minzu University, Enshi, 445000, China

* **Correspondence:** Email: yangyi@sanxiau.edu.cn (Yi Yang), yang1595@126.com (Yi Yang), xcc7426681@126.com (Changcheng Xiang).

Abstract: We investigated the phenomenon of pseudo-Hopf bifurcation in a Filippov Hindmarsh-Rose neuronal system with threshold switching, and the existence of crossing limit cycles was proved by constructing the half-return mapping. Through the threshold control, the firing state of the system could be switched, allowing transitions from a non-periodic state to a periodic state, as well as the evolution from spiking to bursting. Furthermore, through threshold switching, the system exhibited the coexistence of multiple attractors, the system could be in multiple stable states, or have multiple stable sets that could attract system trajectories. This meant that neuronal system could exhibits diverse dynamical behaviors than being limited to a single stable state. The phenomenon of period-doubling bifurcation also indicated that the system will eventually enter a chaotic state. By extending the analysis to nonlinear neuronal systems, this study contributes to a deeper understanding of complex dynamics and provides valuable insights for designing state switching in the application of neural dynamics.

Keywords: Hindmarsh-Rose; pseudo-Hopf bifurcation; crossing limit cycle; Filippov neuronal system; double-tangency singularity

1. Introduction

Hopf bifurcation is a classic phenomenon in nonlinear dynamics. It occurs when an unstable equilibrium point in a system transitions to a stable or unstable limit cycle oscillation at a specific

parameter value. This bifurcation has wide-ranging applications in fields such as biology, physics, chemistry, and engineering. This periodic oscillation phenomenon is commonly observed in many natural and engineering systems, such as biological rhythms and circuit oscillations. In the field of signal processing, Hopf bifurcation is used to explain the interaction between signals and analyze their frequency characteristics. During Hopf bifurcation, characteristic values appear in conjugate complex pairs with a real part of zero. At the bifurcation point, these characteristic values cross the imaginary axis, resulting in the emergence of periodic solutions in the system. For further information on Hopf bifurcation, you can refer to the literature [1–4].

Filippov systems are a type of nonsmooth dynamical system that exhibit multiple regions in their state space. The dynamic equations of the system are smooth in each region. However, the dynamic equations may experience abrupt changes when transitioning among different regions [5–9]. Filippov systems, characterized by their nonsmooth and discontinuous nature, exhibit distinct characteristics in generating bifurcation phenomena. Among these, the pseudo-Hopf bifurcation is commonly observed in Filippov systems, as demonstrated by many studies [2, 10–13]. It is called "pseudo-Hopf bifurcation" because its discontinuity differs from that of a true Hopf bifurcation. The pseudo-Hopf bifurcation is a process where a crossing limit cycle is created, such a orbit intersecting transversally the discontinuous boundary at least twice. However, despite its significance, a formal demonstration of this phenomenon is not provided in [6]. The pseudo-Hopf bifurcation indeed finds various application fields, including dynamical systems, control engineering, and pattern recognition. The pseudo-Hopf bifurcation can be used to describe nonlinear oscillatory phenomena, such as circuit oscillators and stability analysis of mechanical systems. It also plays a role in control system design, aiding in determining system stability, dynamic behavior, and periodic oscillations for optimizing control algorithms. In the domain of pattern recognition, the pseudo-Hopf bifurcation can be utilized to analyze the periodic structures and phase transitions of signals. Overall, the pseudo-Hopf bifurcation provides a tool for understanding and analyzing periodic phenomena and dynamic behavior in complex systems.

The pseudo-Hopf bifurcation have primarily concentrated on identifying multiple limit cycles crossings, The existence of crossing limit cycles with various types of equilibrium points have been considered in many non-smooth systems [10, 13–19]. Liping Li offers a equivalent canonical form to prove the existence of limit cycles in a planar Filippov system, revealing that three crossing limit cycles can originate from the singularities of the discontinuous saddle-focus type [14]. Enrique Ponce et al. demonstrate the emergence of limit cycles via the focus-saddle bifurcation by investigating the oscillation behavior in an electronic circuit containing a single memristor cell [15]. Wang et al. investigate the number of limit cycles in a general planar piecewise linear differential system of saddle-focus type using a Liénard-like canonical form [16]. Huan SongMei investigate the existence and number of limit cycles in a class of general planar piecewise linear systems consisting of two linear subsystems with saddle-saddle dynamics [17], and they also furtherly study the the number of limit cycles in planar piecewise linear systems of node–node types [18]. Wang Jiafu et al. study the number and stability of limit cycles for planar piecewise linear systems of node-saddle type [19]. For more knowledge about crossing limit cycle, readers can refer to the literature [20–27].

In the study of limit cycles, it is frequently observed that multiple cycles emerge through the collision of two invisible tangencies, this singularity is referred to as the Teixeira singularity [13, 28–31]. A. Colombo et al. [28] discussed the Teixeira singularity in discontinuous control systems, providing analytical conditions to study its existence. It is noted that this singularity is present only in MIMO

systems of the Lur'e form. The Teixeira singularity's presence in real applications promises to aid in the design of robust and efficient controllers. A. Colombo and M. R. Jeffrey [29] reviewed the local description of a two-fold singularity formed when a three-dimensional piecewise smooth vector field is tangent to both sides of a switching manifold. Their analysis centered on the dynamics of orbits within sliding regions and identified the conditions under which a pseudoequilibrium traverses the singularity. This represents a novel bifurcation that is fundamentally different from the well-known boundary equilibrium bifurcations in Filippov systems, as it involves a collision between a pseudoequilibrium and a boundary of a sliding or escaping region. The researchers [30] modeled a DC-DC boost converter controlled using a sliding mode control strategy as a discontinuous piecewise linear system, and under certain circuit parameter conditions, the analyzed model may exhibit a Teixeira singularity-bifurcation. This bifurcation can occur in two different forms: supercritical and subcritical. The supercritical case is particularly significant as it pertains to the desired operating point of the boost converter. In their work presented in [31], they filled a gap in both practical and theoretical aspects with a computational procedure. They proposed and detailed a canonical form for discontinuous piecewise linear systems, characterized the topological type of degeneration, and clarified the need for third-order terms in return maps.

However, researchers focusing on the crossing limit cycles have primarily focused on linear systems and demonstrated limited practical applications. Our goal is to extend the analysis to nonlinear neuronal system incorporating Teixeira singularities. Neuronal systems exhibit a wide range of firing patterns, and by implementing threshold control, the system can more easily switch among different firing states, thereby influencing the system's trajectory and firing peak. In neuronal systems, "crossing limit cycle" typically refers to the neurons's periodic firings, such as spiking or bursting, which cross two or more subregions within the system. This paper is based on a single neuron model, but it will be necessary to consider the interactions among multiple nodes in networks in the future to explore more complex phenomena, such as [32–36]. Different nodes adopt different threshold switching strategies, or consider a dual threshold strategy within the same node, which divides thresholds into upper and lower thresholds. Thresholds exhibit complex behavior in individual nodes, and in neural networks, the control of thresholds becomes more intricate due to interactions among nodes.

2. An overview of Filippov systems in $\mathbb{R}^3$

Let us consider a generic 3D-Filippov system expressed by

$$\dot{x} = \begin{cases} g^-(x) = A_1 x + b_1 & \text{if} \quad h(x) < 0, \\ g^+(x) = A_2 x + b_2 & \text{if} \quad h(x) > 0, \end{cases} \tag{2.1}$$

such that $\mathbb{R}^3 = \Sigma^- \cup \Sigma \cup \Sigma^+$, where

$$\Sigma = \left\{ x \in \mathbb{R}^3 : h(x) = \omega^T x - c_0 = 0 \right\},$$

$x = (x_1, x_2, x_3)^T$, $A_1, A_2 \in M_{3\times 3}$, $b_1, b_2, \omega \in \mathbb{R}^3$, and $c_0 \in \mathbb{R}$. Σ denotes the switching manifold.

The switching manifold Σ can be divided into regions with distinct dynamical behaviors: (i) crossing regions (Σ_c), where one vector field points towards Σ, the other points away from the manifold; (ii) attractive sliding regions (Σ_{as}), where both vector fields $g^+$and g^- point towards Σ from opposite sides;

(iii) repulsive sliding regions (Σ_{rs}), where both vector fields g^+ and g^- point away from Σ from opposite sides. Therefore, we differentiate the following regions on Σ:

$$\begin{aligned}
\text{(i)}\Sigma_c &= \left\{x \in \Sigma : \left(\omega^T g^-(x)\right)\left(\omega^T g^+(x)\right) > 0\right\};\\
\text{(ii)}\Sigma_{as} &= \left\{x \in \Sigma : \omega^T g^+(x) < 0 < \omega^T g^-(x)\right\};\\
\text{(iii)}\Sigma_{rs} &= \left\{x \in \Sigma : \omega^T g^-(x) < 0 < \omega^T g^+(x)\right\}.
\end{aligned}$$

When $x \in \Sigma_{as} \cup \Sigma_{rs}$, we define the sliding vector field. Following Filippov's convention [5], the sliding vector field associated with system (2.1) is denoted as g^s and is tangent to Σ. It can be calculated using the formula

$$g^s(x) = \frac{\left(\omega^T g^-(x)\right) g^+(x) - \left(\omega^T g^+(x)\right) g^-(x)}{\omega^T \left(g^-(x) - g^+(x)\right)}. \tag{2.2}$$

Let us define the planes $\pi_i = \left\{x \in \mathbb{R}^3 : \omega^T \left(A_i x + b_i\right) = 0\right\}$, for $i = 1, 2$. These planes intersect with the switching plane Σ, resulting in tangency lines $L_i = \pi_i \cap \Sigma$, for $i = 1, 2$. If these lines intersect transversely, there will be a point $\hat{x} \in \Sigma$ where tangencies occur on both sides of Σ. This point is called a double-tangency singularity. Therefore, the existence of a double tangency singularity in system (2.1) is determined by the existence of a unique solution to the algebraic system

$$Tx = b, \quad T = \begin{pmatrix} \omega^T \\ \omega^T A_1 \\ \omega^T A_2 \end{pmatrix}, \quad b = \begin{pmatrix} c_0 \\ -\omega^T b_1 \\ -\omega^T b_2 \end{pmatrix}.$$

To classify the tangency points, we compute the successive derivatives of $h(x)$ with respect to time at the contact point.

Definition 1. *A tangency point $p \in \Sigma$ is a fold singularity of system* (2.1) *if either*
(i) $\omega^T g^-(p) = 0$ and $\omega^T A_1 g^-(p) \neq 0$ or
(ii) $\omega^T g^+(p) = 0$ and $\omega^T A_2 g^+(p) \neq 0$.
A tangency point $p \in \Sigma$ is a cusp singularity of system (2.1) *if either*
(i) $\omega^T A_1 g^-(p) = 0$ and $\omega^T A_1^2 g^-(p) \neq 0$ or
(ii) $\omega^T A_2 g^+(p) = 0$ and $\omega^T A_2^2 g^+(p) \neq 0$.

Definition 2. *A fold singularity can be classified as visible or invisible, as follows:*
(i) $p \in \Sigma$ is an invisible (visible) fold singularity for f^- if

$$\omega^T f^-(p) = 0 \text{ and } \omega^T A_1 f^-(p) > 0 (< 0).$$

(ii) $p \in \Sigma$ is an invisible (visible) fold singularity for f^+ if

$$\omega^T f^+(p) = 0 \text{ and } \omega^T A_2 f^+(p) < 0 (> 0).$$

A double-tangency singularity that exhibits quadratic tangency on both sides is termed a two-fold singularity. In particular, when the tangency on both sides is invisible, this specific two-fold singularity is referred to as a Teixeira singularity.

We assume that system (2.1) satisfies the following generic hypothesis:

($\mathbf{H_1}$) rank$(T) = 3$, based on hypothesis (H_1), the tangency lines L_1 and L_2 intersect at a unique double-tangency singularity $\hat{x}$.

Lemma 1. *[13] According to the assumption (H_1), the mapping defined by*

$$y = f(x) = T(x - \hat{x}), \tag{2.3}$$

where $T = \begin{pmatrix} \omega^T \\ \omega^T A_1 \\ \omega^T A_2 \end{pmatrix}$ *and $\hat{x}$ the double-tangency singularity, changes the differential system* (2.1) *into the following system*

$$\dot{y} = \begin{cases} \tilde{g}^-(y) = \tilde{A}_1 y + \tilde{b}_1 & \text{if} \quad y_1 < 0, \\ \tilde{g}^+(y) = \tilde{A}_2 y + \tilde{b}_2 & \text{if} \quad y_1 > 0, \end{cases} \tag{2.4}$$

where $\tilde{A}_1 = \begin{pmatrix} 0 & 1 & 0 \\ c_1 & c_2 & c_3 \\ c_4 & c_5 & c_6 \end{pmatrix}$, $\tilde{A}_2 = \begin{pmatrix} 0 & 0 & 1 \\ d_1 & d_2 & d_3 \\ d_4 & d_5 & d_6 \end{pmatrix}$, $\tilde{b}_1 = \begin{pmatrix} 0 \\ r_1 \\ s_1 \end{pmatrix}$, *and* $\tilde{b}_2 = \begin{pmatrix} 0 \\ s_2 \\ r_2 \end{pmatrix}$, *with* $r_i = \omega^T A_i (A_i \hat{x} + b_i)$, *for* $i = 1, 2$.

The following lemma demonstrates the Σ-equivalence property when applying the coordinate transformation (2.3).

Lemma 2. *[13]* $f(\Sigma_u) = \tilde{\Sigma}_u$, *for* $u \in \{as, rs, c\}$.

The lemma presented below establishes the topological equivalence between the new sliding vector field $\tilde{g}_s(y)$ defined in $\tilde{\Sigma}_s$ and the original sliding vector field $g_s(x)$.

Lemma 3. *[13]* $\tilde{g}_s(y) = T g_s(x)$, *for* $x \in \Sigma_s$ *and* $y \in \tilde{\Sigma}_s$.

Proof. Let $y \in \tilde{\Sigma}_s$ be, that is,

$$y = \begin{pmatrix} 0 \\ y_2 \\ y_3 \end{pmatrix} = \begin{pmatrix} 0 \\ \omega^T A_1 (x - \hat{x}) \\ \omega^T A_2 (x - \hat{x}) \end{pmatrix},$$

where $x \in \Sigma_s$. Next, by formula (2.2),

$$\tilde{g}_s(y) = \frac{\left(e_1^T \tilde{g}^-(y)\right) \tilde{g}^+(y) - \left(e_1^T \tilde{g}^+(y)\right) \tilde{g}^-(y)}{e_1^T \left(\tilde{g}^-(y) - \tilde{g}^+(y)\right)}, \tag{2.5}$$

besides, based on Lemma 2 , we have

$$e_1^T \tilde{g}^{\mp}(y) = \omega^T g^{\mp}(x),$$

where $e_1^T = (1, 0, 0)$, $e_2^T = (0, 1, 0)$, $e_3^T = (0, 0, 1)$ and considering that

$$\dot{y} = T\dot{x} \quad \Leftrightarrow \quad \tilde{g}^{\mp}(y) = T g^{\mp}(x),$$

then formula (2.5) is rewritten as

$$\tilde{g}_s(y) = \frac{\left(\omega^T g^-(x)\right) T g^+(x) - \left(\omega^T g^+(x)\right) T g^-(x)}{\omega^T \left(g^-(x) - g^+(x)\right)} = T g_s(x).$$

The proof is completed.

Lemma 4. *[13] Consider the Poincaré map given by the composition of the left-return map φ^- and the right-return map φ^+ (see Appendix A for details). That is, $\Omega : \{\tilde{\Sigma} : u, v < 0\} \mapsto \{\tilde{\Sigma} : u, v < 0\}$ given by*

$$\Omega(u, v, \mu) = \varphi^+ \left(\varphi^-(u, v, \mu)\right) = \begin{pmatrix} \Omega_1(u, v, \mu) \\ \Omega_2(u, v, \mu) \end{pmatrix},$$

where Ω_1 and Ω_2 are given as Taylor series at $u = v = 0$ by

$$\begin{aligned}
\Omega_1(u, v, u) = &\left(\frac{4 s_2 s_\mu}{r_1 r_\mu} - 1\right) u - \frac{2 s_2}{r_\mu} v + \left[\frac{4 s_2 \left(c_6 r_1 - c_3 s_\mu\right)}{r_1^2 r_\mu} + \frac{2\left(d_2 r_\mu - d_5 s_2\right)}{r_\mu^2}\right. \\
&- \left.\frac{8 s_2 s_\mu \left((3 d_2 + d_6) r_\mu - 2 d_5 s_2\right)}{3 r_1 r_u^3}\right] uv + \left[\frac{2\left(c_2 r_1 + c_3 s_\mu\right)}{3 r_1^2}\right. \\
&- \frac{4 s_2 s_\mu (c_2 r_1 + 3 c_6 r_1 - 2 c_3 s_\mu)}{3 r_1^3 r_\mu} - \frac{4 s_\mu \left(d_2 r_\mu - d_5 s_2\right)}{r_1 r_\mu^2} \\
&+ \left.\frac{8 s_2 s_\mu^2 \left((3 d_2 + d_6) r_\mu - 2 d_5 s_2\right)}{3 r_1^2 r_\mu^3}\right] u^2 + \frac{2 s_2 \left((3 d_2 + d_6) r_\mu - 2 d_5 s_2\right)}{3 r_\mu^3} v^2 + \cdots
\end{aligned}$$

$$\begin{aligned}
\Omega_2 (u, v, \mu) = &\frac{2 s_\mu}{r_1} u - v + \left[\frac{2\left(c_6 r_1 - c_3 s_\mu\right)}{r_1^2} - \frac{8 s_\mu \left(d_5 s_2 + d_6 r_\mu\right)}{3 r_1 r_\mu^2}\right] uv \\
&+ \left[\frac{8 s_\mu^2 \left(d_5 s_2 + d_6 r_\mu\right)}{3 r_1^2 r_\mu^2} - \frac{2 s_\mu \left(c_2 r_1 + 3 c_6 r_1 - 2 c_3 s_\mu\right)}{3 r_1^3}\right] u^2 \\
&+ \frac{2\left(d_5 s_2 + d_6 r_\mu\right)}{3 r_\mu^2} v^2 + \cdots
\end{aligned}$$

Then the fixed points (u, v) of this Poincaré map are determined by the following formula

$$\begin{cases} \Omega_1(u, v, \mu) = u, \\ \Omega_2(u, v, \mu) = v. \end{cases}$$

The sliding vector field $\tilde{g}_s(y)$ has the form

$$\tilde{g}_s(y) = \frac{\tilde{g}_r(y)}{\tilde{\Delta}(y)},$$

where $\tilde{g}_r(y)$ is

$$\begin{aligned}
\tilde{g}_r(y) &= e_1^T \left[\begin{pmatrix} 0 & 1 & 0 \\ c_1 & c_2 & c_3 \\ c_4 & c_5 & c_6 \end{pmatrix} \begin{pmatrix} 0 \\ y_2 \\ y_3 \end{pmatrix} + \begin{pmatrix} 0 \\ r_1 \\ s_1 \end{pmatrix} \right] \times \left[\begin{pmatrix} 0 & 0 & 1 \\ d_1 & d_2 & d_3 \\ d_4 & d_5 & d_6 \end{pmatrix} \begin{pmatrix} 0 \\ y_2 \\ y_3 \end{pmatrix} + \begin{pmatrix} 0 \\ s_2 \\ r_2 \end{pmatrix} \right] \\
&\quad - e_1^T \left[\begin{pmatrix} 0 & 0 & 1 \\ d_1 & d_2 & d_3 \\ d_4 & d_5 & d_6 \end{pmatrix} \begin{pmatrix} 0 \\ y_2 \\ y_3 \end{pmatrix} + \begin{pmatrix} 0 \\ s_2 \\ r_2 \end{pmatrix} \right] \left[\begin{pmatrix} 0 & 1 & 0 \\ c_1 & c_2 & c_3 \\ c_4 & c_5 & c_6 \end{pmatrix} \begin{pmatrix} 0 \\ y_2 \\ y_3 \end{pmatrix} + \begin{pmatrix} 0 \\ r_1 \\ s_1 \end{pmatrix} \right] \\
&= e_1^T \begin{pmatrix} y_2 \\ c_2 y_2 + c_3 y_3 + r_1 \\ c_5 y_2 + c_6 y_3 + s_1 \end{pmatrix} \begin{pmatrix} y_3 \\ d_2 y_2 + d_3 y_3 + s_2 \\ d_5 y_2 + d_6 y_3 + r_2 \end{pmatrix} - e_1^T \begin{pmatrix} y_3 \\ d_2 y_2 + d_3 y_3 + s_2 \\ d_5 y_2 + d_6 y_3 + r_2 \end{pmatrix} \begin{pmatrix} y_2 \\ c_2 y_2 + c_3 y_3 + r_1 \\ c_5 y_2 + c_6 y_3 + s_1 \end{pmatrix} \\
&= y_2 \begin{pmatrix} y_3 \\ d_2 y_2 + d_3 y_3 + s_2 \\ d_5 y_2 + d_6 y_3 + r_2 \end{pmatrix} - y_3 \begin{pmatrix} y_2 \\ c_2 y_2 + c_3 y_3 + r_1 \\ c_5 y_2 + c_6 y_3 + s_1 \end{pmatrix} \\
&= \begin{pmatrix} 0 \\ d_2 y_2^2 + (d_3 - c_2) y_2 y_3 - c_3 y_3^2 + s_2 y_2 - r_1 y_3 \\ d_5 y_2^2 + (d_6 - c_5) y_2 y_3 - c_6 y_3^2 + r_2 y_2 - s_1 y_3 \end{pmatrix}
\end{aligned}$$

and $\tilde{\Delta}(y)$ is

$$\tilde{\Delta}(y) = e_1^T \left(\tilde{g}^-(y) - \tilde{g}^+(y) \right) = \begin{pmatrix} 1 & 0 & 0 \end{pmatrix} \left[\begin{pmatrix} y_2 \\ (\cdot) \\ (\cdot) \end{pmatrix} - \begin{pmatrix} y_3 \\ (\cdot) \\ (\cdot) \end{pmatrix} \right] = y_2 - y_3.$$

To simplify and facilitate numerical simulation implementation, we will consider a two-dimensional system in this paper.

For the pseudo-Hopf bifurcation to occur, it is necessary for system (2.1) to satisfy another hypothesis:

(**$\mathbf{H_2}$**) There exists a parameter ε such that for the critical value $\varepsilon = \varepsilon_0$, the vector fields $g^{\mp}(x, \varepsilon)$ satisfy the condition $g^+(\hat{x}, \varepsilon_0) = kg^-(\hat{x}, \varepsilon_0)$, with $k < 0$.

In light of hypothesis (H_2), the vector fields $g^{\mp}(x, \varepsilon)$ exhibit antiparallel behavior at the Teixeira singularity when the bifurcation parameter ε reaches the critical value ε_0. Recent studies have shown that this condition is necessary for the emergence of a crossing limit cycle as the parameter transitions away from ε_0.

By Eq (2.4), it can be derived that

$$\tilde{f}^+(0, \varepsilon_0) = k\tilde{f}^-(0, \varepsilon_0), \quad k < 0,$$

thus,

$$s_2(\varepsilon_0) = kr_1(\varepsilon_0) \text{ and } r_2(\varepsilon_0) = ks_1(\varepsilon_0).$$

We can assume that $k = \frac{r_2(\varepsilon_0)}{s_1(\varepsilon_0)}$, subsequently,

$$\tilde{f}^-(0, \varepsilon_0) = \begin{pmatrix} 0 \\ r_1(\varepsilon_0) \\ s_1(\varepsilon_0) \end{pmatrix} \text{ and } \tilde{f}^+(0, \varepsilon_0) = \begin{pmatrix} 0 \\ \frac{r_1(\varepsilon_0) r_2(\varepsilon_0)}{s_1(\varepsilon_0)} \\ r_2(\varepsilon_0) \end{pmatrix}.$$

In other words, by perturbing the constant components of the vector fields in the normal form (2.4), we can disrupt the antiparallel behavior. To achieve this, we consider the unfolding of the system

$$\dot{y} = \begin{cases} \begin{pmatrix} 0 & 1 & 0 \\ c_1 & c_2 & c_3 \\ c_4 & c_5 & c_6 \end{pmatrix} y + \begin{pmatrix} 0 \\ r_1 \\ s_1 + \mu \end{pmatrix} & \text{if } y_1 < 0, \\ \begin{pmatrix} 0 & 0 & 1 \\ d_1 & d_2 & d_3 \\ d_4 & d_5 & d_6 \end{pmatrix} y + \begin{pmatrix} 0 \\ \frac{r_1 r_2}{s_1} \\ r_2 + \mu \end{pmatrix} & \text{if } y_1 > 0. \end{cases} \tag{2.6}$$

3. The existence of crossing limit cycle

Theorem 1. *Consider the unfolding system* (2.6)*. Since* $r_1 > 0, r_2 < 0$ *and* $s_1 > 0$*, then system* (2.6) *has a crossing limit cycle for* $\mu\,(3r_2\varepsilon_1 + r_1\varepsilon_2) > 0$ *and* μ *sufficiently small, where*

$$\begin{aligned} \varepsilon_1 &= c_6 d_5 r_1^3 + c_6 d_6 r_1^2 s_1 - c_2 c_6 r_1^2 r_2 - c_3 c_6 r_1 r_2 s_1 + c_2 c_3 r_1 r_2 s_1 + c_3^2 r_2 s_1^2, \\ \varepsilon_2 &= 2c_2 d_5 r_1^2 r_2 + 2c_2 d_6 r_1 r_2 s_1 - 2d_5^2 r_1^3 - 2d_6^2 r_1 s_1^2 - 4d_5 d_6 r_1^2 s_1 - c_3 d_5 r_1 r_2 s_1 - c_3 d_6 r_2 s_1^2, \end{aligned}$$

furtherly, since $u < -\frac{2}{\theta_1+\theta_2}(-\frac{2}{\theta_1+\theta_2} < u < 0)$*, where* u *is defined by Poincaré map* (5.11)*, the crossing limit cycle is stable(unstable) of node type if*

$$\begin{gathered} \theta_1 + \theta_2 > 0, \quad \theta_1\theta_2 > \theta_3\theta_4, \quad 3\theta_2 - \theta_1 + 2(\frac{r_1}{s_1}\theta_4 - \frac{s_1}{r_1}\theta_3) < 0, \\ (\theta_1 + \theta_2)^2 > 4\,(\theta_1\theta_2 - \theta_3\theta_4)\,, \quad (\theta_1 - \theta_2) < \left(\frac{r_1}{s_1}\theta_4 - \frac{s_1}{r_1}\theta_3\right), \end{gathered}$$

since $u < -\frac{2}{\theta_1+\theta_2}(-\frac{2}{\theta_1+\theta_2} < u < 0)$*, the crossing limit cycle is stable(unstable) of focus type if*

$$\begin{gathered} \theta_1 + \theta_2 > 0, \quad \theta_1\theta_2 > \theta_3\theta_4, \quad 3\theta_2 - \theta_1 + 2(\frac{r_1}{s_1}\theta_4 - \frac{s_1}{r_1}\theta_3) < 0, \\ (\theta_1 + \theta_2)^2 < 4\,(\theta_1\theta_2 - \theta_3\theta_4)\,, \quad (\theta_1 - \theta_2) > \left(\frac{r_1}{s_1}\theta_4 - \frac{s_1}{r_1}\theta_3\right), \end{gathered}$$

since $u < 0$ *the crossing limit cycle is of saddle type if*

$$\theta_1\theta_2 > \theta_3\theta_4, \quad 3\theta_2 - \theta_1 + 2(\frac{r_1}{s_1}\theta_4 - \frac{s_1}{r_1}\theta_3) > 0,$$

where $\theta_1, \theta_2, \theta_3, \theta_4$ *are defined in expression* (3.6)*.*

Proof. We define the functions

$$\begin{aligned} P_1(u, v, \mu) &= \Omega_1(u, v, \mu) - u, \\ P_2(u, v, \mu) &= \Omega_2(u, v, \mu) - v. \end{aligned} \tag{3.1}$$

where $\Omega_1(u, v, \mu)$ and $\Omega_2(u, v, \mu)$ are defined by Lemma 4. Hence, solving (3.1) is identical to solving $P_1(u, v, \mu) = 0$ and $P_2(u, v, \mu) = 0$. Substituting $s_\mu = s_1 + \mu$, $r_\mu = r_2 + \mu$ and $s_2 = \frac{r_1 r_2}{s_1}$ in to P_1, it is obvious that

$$P_1(0, 0, 0) = 0 \quad \text{and} \quad \frac{\partial P_1}{\partial v}(0, 0, 0) = -\frac{2r_1}{s_1}.$$

then, by the implicit function theorem (IFT), there exists a function $\rho(u,\mu)$ such that $P_1(u,\rho(u,\mu),\mu)\equiv 0$ in a neighborhood of $(0,0,0)$. This function is defined by

$$v=\rho(u,\mu)=a_{1\mu}u+a_{2\mu}u^2+\mathscr{O}\left(|u|^3\right). \tag{3.2}$$

Substituted into P_1

$$\begin{aligned}
P_1(u,v,\mu)&=\Omega_1(u,v,\mu)-u\\
&=\left(\frac{4s_2s_\mu}{r_1r_\mu}-2\right)u-\frac{2s_2}{r_\mu}\left(a_{1\mu}u+a_{2\mu}u^2+\cdots\right)\\
&\quad+\Big[\frac{2\left(c_2r_1+c_3s_\mu\right)}{3r_1^2}-\frac{4s_2s_\mu(c_2r_1+3c_6r_1-2c_3s_\mu)}{3r_1^3r_\mu}\\
&\qquad-\frac{4s_\mu\left(d_2r_\mu-d_5s_2\right)}{r_1r_\mu^2}+\frac{8s_2s_\mu^2(\,(3d_2+d_6)\,r_\mu-2d_5s_2)}{3r_1^2r_\mu^3}\Big]u^2\\
&\quad+\Big[\frac{4s_2\left(c_6r_1-c_3s_\mu\right)}{r_1^2r_\mu}+\frac{2\left(d_2r_\mu-d_5s_2\right)}{r_\mu^2}\\
&\qquad-\frac{8s_2s_\mu(\,(3d_2+d_6)\,r_\mu-2d_5s_2)}{3r_1{r_\mu}^3}\Big]\times u\left(a_{1\mu}u+a_{2\mu}u^2+\cdots\right)\\
&\quad+\frac{2s_2(\,(3d_2+d_6)\,r_\mu-2d_5s_2)}{3r_\mu^3}\left(a_{1\mu}u+a_{2\mu}u^2+\cdots\right)^2\\
&=\left(\frac{4s_2s_\mu}{r_1r_\mu}-\frac{2s_2}{r_\mu}a_{1\mu}-2\right)u+\left[\delta_1+\delta_2a_{1\mu}+\delta_3a_{1\mu}^2-\frac{2s_2}{r_\mu}a_{2\mu}\right]u^2+\cdots
\end{aligned}$$

where

$$\begin{aligned}
\delta_1&=\Big[\frac{2\left(c_2r_1+c_3s_\mu\right)}{3r_1^2}-\frac{4s_2s_\mu(c_2r_1+3c_6r_1-2c_3s_\mu)}{3r_1^3r_\mu}-\frac{4s_\mu\left(d_2r_\mu-d_5s_2\right)}{r_1r_\mu^2}+\frac{8s_2s_\mu^2(\,(3d_2+d_6)\,r_\mu-2d_5s_2)}{3r_1^2r_\mu^3}\Big],\\
\delta_2&=\Big[\frac{4s_2\left(c_6r_1-c_3s_\mu\right)}{r_1^2r_\mu}+\frac{2\left(d_2r_\mu-d_5s_2\right)}{r_\mu^2}-\frac{8s_2s_\mu(\,(3d_2+d_6)\,r_\mu-2d_5s_2)}{3r_1{r_\mu}^3}\Big],\\
\delta_3&=\frac{2s_2(\,(3d_2+d_6)\,r_\mu-2d_5s_2)}{3r_\mu^3},
\end{aligned}$$

for $P_1\equiv 0$, thus,

$$\frac{4s_2s_\mu}{r_1r_\mu}-\frac{2s_2}{r_\mu}a_{1\mu}-2=0,\quad \delta_1+\delta_2a_{1\mu}+\delta_3a_{1\mu}^2-\frac{2s_2}{r_\mu}a_{2\mu}=0,$$

therefore,

$$a_{1\mu}=\frac{r_2\,(s_1+2\mu)-s_1\mu}{r_1r_2},\quad a_{2\mu}==\frac{s_1\left(d_5r_1^2+d_6s_1r_1-c_2r_1r_2-c_3s_1r_2\right)}{3r_1^3r_2}.$$

Next, we substitute (3.2) into P_2, resulting in

$$
\begin{aligned}
P_2(u,\rho(u,\mu),\mu) =& \left[\frac{2s_1}{r_1} - \frac{2r_2s_1 + 4r_2\mu - 2s_1\mu}{r_1r_2}\right]u + \left[\frac{6r_2^2(c_6r_1 - c_3s_1) - 8s_1r_1(d_5s_2 + d_6r_2)}{3r_1^2r_2^2}\right.\\
&\times \frac{r_2s_1 + 2r_2\mu - s_1\mu}{r_1r_2} - \frac{2s_1(d_5r_1^2 + d_6s_1r_1 - c_2r_1r_2 - c_3s_1r_2)}{3r_1^3r_2}\\
&+ \frac{8s_1^2r_1\,(d_5s_2 + d_6r_2) - 2s_1r_2^2\,(c_2r_1 + 3c_6r_1 - 2c_3s_1)}{3r_1^3r_2^2} + \frac{2\,(d_5s_2 + d_6r_2)}{3r_2^2}\\
&\left.\times \frac{(r_2\,(s_1 + 2\mu) - s_1\mu)^2}{r_1^2r_2^2}\right]u^2 + \left[\frac{6r_2^2\,(c_6r_1 - c_3s_1) - 8s_1r_1\,(d_5s_2 + d_6r_2)}{3r_1^2r_2^2}\right.\\
&\times \frac{s_1\left(d_5r_1^2 + d_6s_1r_1 - c_2r_1r_2 - c_3s_1r_2\right)}{3r_1^3r_2} + \frac{2\,(d_5s_2 + d_6r_2)}{3r_2^2}\\
&\left.\times \frac{2\Big(r_2\,(s_1 + 2\mu) - s_1\mu\Big)\Big(s_1\left(d_5r_1^2 + d_6s_1r_1 - c_2r_1r_2 - c_3s_1r_2\right)\Big)}{r_1r_2 \times 3r_1^3r_2}\right]u^3 + \cdots\\
=& \frac{-18\,(2r_2 - s_1)\,r_1^4r_2^3}{9r_1^5r_2^4}\mu u + \left[\frac{3\Delta_1\,(2r_2 - s_1)\,r_1^2r_2}{9r_1^5r_2^4} + \frac{3\Delta_4\,(2r_2s_1\,(2r_2 - s_1))\,r_1^3}{9r_1^5r_2^4}\right]\mu u^2\\
&+ \frac{2\Delta_2\Delta_4\,(2r_2 - s_1)\,r_1}{9r_1^5r_2^4}\mu u^3 + \left[\frac{3\Delta_1s_1r_1^2r_2^2}{9r_1^5r_2^4} + \frac{3\Delta_3r_1^2r_2^2}{9r_1^5r_2^4} + \frac{3\Delta_4s_1^2r_1^3r_2^2}{9r_1^5r_2^4} - \frac{6\Delta_2r_1^2r_2^3}{9r_1^5r_2^4}\right]u^2\\
&+ \left[\frac{\Delta_1\Delta_2r_2}{9r_1^5r_2^4} + \frac{2\Delta_2\Delta_4s_1r_1r_2}{9r_1^5r_2^4}\right]u^3 + \cdots
\end{aligned}
$$

where

$$
\begin{aligned}
&\Delta_1 = 6r_2^2\,(c_6r_1 - c_3s_1) - 8s_1r_1\,(d_5s_2 + d_6r_2)\,, \quad \Delta_2 = s_1\left(d_5r_1^2 + d_6s_1r_1 - c_2r_1r_2 - c_3s_1r_2\right),\\
&\Delta_3 = 8s_1^2r_1\,(d_5s_2 + d_6r_2) - 2s_1r_2^2\,(c_2r_1 + 3c_6r_1 - 2c_3s_1)\,, \quad \Delta_4 = 2\,(d_5s_2 + d_6r_2)\,,
\end{aligned}
$$

thus,

$$
\begin{aligned}
&P_2(u,\rho(u,\mu),\mu) = -\frac{u}{9r_1^5r_2^4}P^*(u,\mu),\\
&P^*(u,\mu) = 18r_1^4r_2^3\,(2r_2 - s_1)\,\mu - M_1u\mu - M_2u^2\mu - M_3u - M_4u^2 + \mathscr{O}\left(|u|^3\right),
\end{aligned}
$$

where

$$
\begin{aligned}
&M_1 = 3r_1^2r_2\,(2r_2 - s_1)\,\Delta_1 + 6r_1^3r_2s_1\,(2r_2 - s_1)\,\Delta_4, \quad M_2 = 2r_1\,(2r_2 - s_1)\,\Delta_2\Delta_4,\\
&M_3 = 3r_1^2r_2^2s_1\Delta_1 + 3r_1^2r_2^2\Delta_3 + 3r_1^3r_2^2s_1^2\Delta_4 - 6r_1^2r_2^3\Delta_2, \quad M_4 = r_2\Delta_1\Delta_2 + 2r_1r_2s_1\Delta_2\Delta_4.
\end{aligned}
$$

Since $P^*(0,0) = 0$ and $\frac{\partial P^*}{\partial \mu}(0,0) = 18r_1^4r_2^3\,(2r_2 - s_1) \neq 0$, so again by the IFT, supposing there exists a function

$$
\mu = h(u) = \epsilon u^2 + \mathscr{O}\left(|u|^3\right), \tag{3.3}
$$

such that $P^*(u,h(u)) = 0$ in a neighborhood of the point $(0,0)$, and $P_2(u,\rho(u,h(u)),h(u)) = 0$ in a neighborhood of the point $(0,0,0)$, substituting into $P^*(u,\mu)$, we could obtain that

$$
\epsilon = \frac{s_1}{9r_1^4r_2\,(2r_2 - s_1)}\,(3r_2\varepsilon_1 + r_1\varepsilon_2)\,, \tag{3.4}
$$

where

$$\varepsilon_1 = c_6d_5r_1^3 + c_6d_6r_1^2s_1 - c_2c_6r_1^2r_2 - c_3c_6r_1r_2s_1 + c_2c_3r_1r_2s_1 + c_3^2r_2s_1^2,$$
$$\varepsilon_2 = 2c_2d_5r_1^2r_2 + 2c_2d_6r_1r_2s_1 - 2d_5^2r_1^3 - 2d_6^2r_1s_1^2 - 4d_5d_6r_1^2s_1 - c_3d_5r_1r_2s_1 - c_3d_6r_2s_1^2.$$

Since $r_1 > 0$, $r_2 < 0$ and $s_1 > 0$, then for every μ sufficiently small with $\mu(3r_2\varepsilon_1 + r_1\varepsilon_2) = \frac{s_1}{9r_1^4r_2(2r_2-s_1)}(3r_2\varepsilon_1 + r_1\varepsilon_2)^2u^2 > 0$, there is a $u < 0$, such that

$$\Omega(u, \rho(u), h(u)) = (u, \rho(u))^T.$$

In other words, a crossing limit cycle has been identified. Finally, to analyze the stability of the CLC, we compute the eigenvalue of the Jacobian matrix of $\Omega(u, \rho(u), h(u))$. The Jacobian matrix of $\Omega(u, \rho(u), h(u))$ is given by

$$D\Omega(u, \rho(u), h(u)) = \begin{pmatrix} \dfrac{4s_2s_\mu}{r_1r_\mu} - 1 + m_1v + 2m_2u, & \dfrac{-2s_2}{r_\mu} + m_1u + 2m_3v \\ \\ \dfrac{2s_\mu}{r_1} + n_1v + 2n_2u, & -1 + n_1u + 2n_3v \end{pmatrix}, \tag{3.5}$$

where

$$m_1 = \frac{4s_2\left(c_6r_1 - c_3s_\mu\right)}{r_1^2r_\mu} + \frac{2\left(d_2r_\mu - d_5s_2\right)}{r_\mu^2} - \frac{8s_2s_\mu\left((3d_2 + d_6)r_\mu - 2d_5s_2\right)}{3r_1r_\mu^3},$$
$$m_2 = \frac{2\left(c_2r_1 + c_3s_\mu\right)}{3r_1^2} - \frac{4s_2s_\mu(c_2r_1 + 3c_6r_1 - 2c_3s_\mu)}{3r_1^3r_\mu} - \frac{4s_\mu\left(d_2r_\mu - d_5s_2\right)}{r_1r_\mu^2} + \frac{8s_2s_\mu^2((3d_2 + d_6)r_\mu - 2d_5s_2)}{3r_1^2r_\mu^3},$$
$$m_3 = \frac{2s_2\left((3d_2 + d_6)r_\mu - 2d_5s_2\right)}{3r_\mu^3},$$
$$n_1 = \frac{2\left(c_6r_1 - c_3s_\mu\right)}{r_1^2} - \frac{8s_\mu\left(d_5s_2 + d_6r_\mu\right)}{3r_1r_\mu^2},$$
$$n_2 = \frac{8s_\mu^2\left(d_5s_2 + d_6r_\mu\right)}{3r_1^2r_\mu^2} - \frac{2s_\mu\left(c_2r_1 + 3c_6r_1 - 2c_3s_\mu\right)}{3r_1^3},$$
$$n_3 = \frac{2\left(d_5s_2 + d_6r_\mu\right)}{3r_\mu^2},$$

thus the eigenvalues are

$$\lambda_{1,2} = 1 + \frac{\theta_1 + \theta_2}{2}u + \mathscr{O}\left(|u|^2\right) \pm \sqrt{\vartheta u + \left[\frac{(\theta_1 + \theta_2)^2}{4} - (\theta_1\theta_2 - \theta_3\theta_4)\right]u^2 + \mathscr{O}\left(|u|^3\right)}, \tag{3.6}$$

where

$$\vartheta = 2(\theta_1 - \theta_2) + 2(\frac{s_1}{r_1}\theta_3 - \frac{r_1}{s_1}\theta_4), \quad \theta_1 = m_1\frac{s_1}{r_1} + 2m_2,$$
$$\theta_2 = n_1 + 2n_3\frac{s_1}{r_1}, \quad \theta_3 = m_1 + 2m_3\frac{s_1}{r_1}, \quad \theta_4 = n_1\frac{s_1}{r_1} + 2n_2.$$

Then, since $u < -\frac{2}{\theta_1+\theta_2}(-\frac{2}{\theta_1+\theta_2} < u < 0)$, the CLC is stable(unstable) of node type if

$$\theta_1 + \theta_2 > 0, \quad \theta_1\theta_2 > \theta_3\theta_4, \quad 3\theta_2 - \theta_1 + 2(\frac{r_1}{s_1}\theta_4 - \frac{s_1}{r_1}\theta_3) < 0,$$
$$(\theta_1 + \theta_2)^2 > 4\left(\theta_1\theta_2 - \theta_3\theta_4\right), \quad (\theta_1 - \theta_2) < \left(\frac{r_1}{s_1}\theta_4 - \frac{s_1}{r_1}\theta_3\right),$$

since $u < -\frac{2}{\theta_1+\theta_2}(-\frac{2}{\theta_1+\theta_2} < u < 0)$, the CLC is stable(unstable) of focus type if

$$\theta_1 + \theta_2 > 0, \quad \theta_1\theta_2 > \theta_3\theta_4, \quad 3\theta_2 - \theta_1 + 2(\frac{r_1}{s_1}\theta_4 - \frac{s_1}{r_1}\theta_3) < 0,$$
$$(\theta_1 + \theta_2)^2 < 4\left(\theta_1\theta_2 - \theta_3\theta_4\right), \quad (\theta_1 - \theta_2) > \left(\frac{r_1}{s_1}\theta_4 - \frac{s_1}{r_1}\theta_3\right),$$

since $u < 0$ the CLC is of saddle type if

$$\theta_1\theta_2 > \theta_3\theta_4, \quad 3\theta_2 - \theta_1 + 2(\frac{r_1}{s_1}\theta_4 - \frac{s_1}{r_1}\theta_3) > 0.$$

The proof is completed.

4. Dynamics and bifurcation for a Hindmarsh and Rose neuronal model

The three-dimensional Hindmarsh Rose neuron model [37] is a mathematical model describing the electrical activity of neurons, which contains three nonlinear differential equations:

$$\begin{aligned} \frac{dx}{dt} &= y - ax^3 + bx^2 - fz + I, \\ \frac{dy}{dt} &= c - dx^2 - y, \\ \frac{dz}{dt} &= r\left(s\left(x - x_0\right) - z\right), \end{aligned} \tag{4.1}$$

the system is described by three variables $x(t)$, $y(t)$, and $z(t)$. These variables represent the membrane potential, spiking variable (fast current), and bursting variable (slow current), respectively. The behavior of these variables is determined by the transport of ions through ion channels present in the membrane. There are several parameters involved in this system, namely a, b, c, d, f, r, s, I, and x_0. Each parameter plays a different role: I determines the level of excitability or external forcing current for biological neurons, b allows the switching between bursting and spiking behaviors and controlling spiking frequency. The parameter r regulates the change rate of the slow variable $z(t)$ and is usually considered to be a small positive real number, Last, x_0 represents the resting potential of the system.

In this paper, on the basis of the above three-dimensional neuron system, we consider taking control strategies to the membrane potential. That is, when variable $x(t)$ does not reach a critical level c_0, b and I may take the larger values denoted by $b_{\max}$ and $I_{\max}$, respectively, otherwise, b and I should take the smaller values, $b_{\min}$ and $I_{\min}$, to make sure $x(t)$ decreases once the membrane potential $x(t)$ is above the threshold c_0. The switching function is given by

$$\begin{cases} b = b_{\max}, & I = I_{\max}, \quad x < \mathrm{c}_0, \\ b = b_{\min}, & I = I_{\min}, \quad x > \mathrm{c}_0. \end{cases} \tag{4.2}$$

The proof of crossing the limit cycle in the previous section applies to linear systems. For nonlinear systems, it cannot be directly applied and it is necessary to transform the nonlinear system into a linear system. In order to linearize this nonlinear system of equations, we need to transform them into a set of linear equations. The specific operation is as follows: First, we perform first-order Taylor expansion on x:

$$x(t+\Delta t) = x(t) + \frac{dx}{dt}\Delta t.$$

Combining the first equation of the system (4.1) yields:

$$x(t+\Delta t) = x(t) + y(t)\Delta t + \left(-ax^3(t) + bx^2(t) - fz(t) + I\right)\Delta t.$$

Perform the first derivative on both sides of the above equation simultaneously to obtain:

$$\frac{x(t+\Delta t) - x(t)}{\Delta t} = y(t) + \left(-3ax^2(t) + 2bx(t) - \frac{fz(t)}{x(t)} + I\right)\frac{\Delta t}{x(t)}.$$

Similarly, we perform first-order Taylor expansions on y and z:

$$y(t+\Delta t) = y(t) + \frac{dy}{dt}\Delta t, \quad z(t+\Delta t) = z(t) + \frac{dz}{dt}\Delta t.$$

Combining the second and third equations of system (4.1) yields:

$$y(t+\Delta t) = y(t) + \left(c - dx^2(t) - y(t)\right)\Delta t, \quad z(t+\Delta t) = z(t) + r\left(s\left(x(t) - x_0\right) - z(t)\right)\Delta t.$$

Perform the first derivative of the above two equations to obtain:

$$\frac{y(t+\Delta t) - y(t)}{\Delta t} = -2x(t)y(t) - y(t) + c, \quad \frac{z(t+\Delta t) - z(t)}{\Delta t} = -rsz(t) + rsx(t).$$

Organize the above several formulas into matrix form:

$$\begin{bmatrix} \frac{x(t+\Delta t)-x(t)}{\Delta t} \\ \frac{y(t+\Delta t)-y(t)}{\Delta t} \\ \frac{z(t+\Delta t)-z(t)}{\Delta t} \end{bmatrix} = \begin{bmatrix} y(t)\frac{\Delta t}{x(t)} \\ \frac{\Delta tc}{2} - \frac{\Delta ty(t)}{2} - \frac{\Delta tx^2(t)}{2} \\ -rsz(t)\Delta t + \frac{rsx(t)\Delta t}{x(t)} \end{bmatrix} + \begin{bmatrix} \left(-3ax^2(t) + 2bx(t) - \frac{fz(t)}{x(t)} + I\right)\frac{\Delta t}{x(t)} \\ \frac{c}{2}\Delta t \\ 0 \end{bmatrix}.$$

Substitute the equilibrium points x_0, y_0, z_0 for $x(t), y(t), z(t)$ respectively in the above equation,

$$\begin{bmatrix} \frac{\Delta x}{\Delta t} \\ \frac{\Delta y}{\Delta t} \\ \frac{\Delta z}{\Delta t} \end{bmatrix} = \begin{bmatrix} 0 & \frac{\Delta t}{x_0} & 0 \\ -\frac{\Delta t}{2} & -1 & 0 \\ \frac{rs\Delta t}{x_0} & 0 & -rs\Delta t \end{bmatrix}\begin{bmatrix} x - x_0 \\ y - y_0 \\ z - z_0 \end{bmatrix} + \begin{bmatrix} \left(-3ax_0^2 + 2bx_0 - \frac{fz_0}{x_0} + I\right)\frac{\Delta t}{x_0} \\ \frac{c}{2}\Delta t \\ 0 \end{bmatrix}, \tag{4.3}$$

replace $x - x_0$, $y - y_0$ and $z - z_0$ with x_1, x_2 and x_3, respectively, the equation above is equivalent to

$$\begin{bmatrix} \frac{dx_1}{dt} \\ \frac{dx_2}{dt} \\ \frac{dx_3}{dt} \end{bmatrix} = \begin{bmatrix} 0 & 1 & 0 \\ -\frac{x_0}{2} & -\frac{x_0}{\Delta t} & 0 \\ rs & 0 & -rsx_0 \end{bmatrix}\begin{bmatrix} x_1 \\ x_2 \\ x_3 \end{bmatrix} + \begin{bmatrix} \left(-3ax_0^2 + 2bx_0 - \frac{fz_0}{x_0} + I\right) \\ \frac{c}{2}x_0 \\ 0 \end{bmatrix}. \tag{4.4}$$

In this way, we obtain the linearized equation of system (4.1). In practical applications, The time step size Δt is usually determined based on the specific problem being studied and the numerical simulation method being used. it should be small enough to ensure numerical convergence to the true solution, it should not be too small to avoid excessive computational cost and time. In this article, Δt is taken as 0.01.

According to system (4.4), we can construct the Filippov system with two zones separated by the switching line $\Sigma = \left\{x \in \mathbb{R}^3 : h(x) = \omega^T x - c_0 = 0\right\}$, where $x = (x_1, x_2, x_3)^T$, $\omega^T = (\omega_1, \omega_2, \omega_3)$, and the corresponding Filippov system can be expressed in the following form:

$$\dot{x} = \begin{cases} g^-(x) = A_1 x + b_1 & \text{if} \quad h(x) < 0, \\ g^+(x) = A_2 x + b_2 & \text{if} \quad h(x) > 0, \end{cases} \tag{4.5}$$

where

$$A_1 = \begin{pmatrix} 0 & 1 & 0 \\ -\frac{x_0}{2} & -\frac{x_0}{\Delta t} & 0 \\ rs & 0 & -rsx_0 \end{pmatrix}, \quad b_1 = \begin{pmatrix} -3ax_0^2 + 2b_{\max}x_0 - \frac{fz_0}{x_0} + I_{\max} \\ \frac{c}{2}x_0 \\ 0 \end{pmatrix},$$

$$A_2 = \begin{pmatrix} 0 & 1 & 0 \\ -\frac{x_0}{2} & -\frac{x_0}{\Delta t} & 0 \\ rs & 0 & -rsx_0 \end{pmatrix}, \quad b_2 = \begin{pmatrix} -3ax_0^2 + 2b_{\min}x_0 - \frac{fz_0}{x_0} + I_{\min} \\ \frac{c}{2}x_0 \\ 0 \end{pmatrix}.$$

Then, according to the mapping $y = f(x) = T(x - \hat{x})$ in Lemma 1 of the second section, we need to calculate T and $\hat{x}$ where $T = \begin{pmatrix} \omega^T \\ \omega^T A_1 \\ \omega^T A_2 \end{pmatrix}$ and $\hat{x}$ is the double-tangency singularity. We can express the following set of equations:

$$\begin{cases} A_1 x + b_1 - \lambda\omega = 0, \\ A_2 x + b_2 - \lambda\omega = 0, \\ \omega^T x - c_0 = 0, \end{cases}$$

here, λ is a Lagrange multiplier. To find the double-tangential singularity $\hat{x}$, we need to transform the above set of equations into a linear system of equations with respect to x. By multiplying the first and second equations with ω^T and subtracting them, we obtain:

$$(A_1 - A_2)\, x + (b_1 - b_2) - (\lambda_1 - \lambda_2)\, \omega = 0.$$

Similarly, by multiplying the first and third equations with A_2 and $-\omega^T$, respectively, and adding them, we can get

$$\left(A_1 + A_2^T\right) x + \left(b_1 - A_2^T \hat{x}\right) - \lambda_1 \omega = 0.$$

By replacing λ_2 with λ_1 in the above equation and substituting it into the previous equation, we obtain

$$(A_1 - A_2)\, x + (b_1 - b_2) + \left(A_2^T \hat{x} - b_1\right) - \lambda_1 \omega = 0.$$

Combining the above two equations yields:

$$\begin{bmatrix} A_1 - A_2 & -(\lambda_1 - \lambda_2)\,\mathbf{I}_3 & 0 \\ A_1 + A_2^T & -\lambda_1 \mathbf{I}_3 & -A_2^T \end{bmatrix} \begin{bmatrix} x \\ \omega \\ \hat{x} \end{bmatrix} = \begin{bmatrix} -(b_1 - b_2) \\ -\left(b_1 - A_2^T \hat{x}\right) \end{bmatrix},$$

where $\mathbf{I}_3$ is 3×3 identity matrix. Solving the above linear system of equations yields expressions for x and $\hat{x}$. Next, we need to determine $\tilde{A}_1, \tilde{A}_2, \tilde{b}_1, \tilde{b}_2$. Based on the mapping $y = f(x) = T(x - \hat{x})$, we can obtain

$$\tilde{A}_1 = TA_1T^{-1}, \quad \tilde{A}_2 = TA_2T^{-1}, \quad \tilde{b}_1 = Tb_1 - \tilde{A}_1\hat{x}, \quad \tilde{b}_2 = Tb_2 - \tilde{A}_2\hat{x},$$

supposing $\hat{x} = (\hat{x_1}, \hat{x_2}, \hat{x_3})$, by substituting the specific forms of A_1, A_2, b_1 and b_2 into the above expressions, we obtain the following expressions for $\tilde{A}_1, \tilde{A}_2, \tilde{b}_1$ and $\tilde{b}_2$,

$$\begin{aligned}
\tilde{A}_1 &= \frac{1}{\omega_1^2 + \omega_2^2 + \omega_3^2} \begin{bmatrix} 0 & \omega_2 & 0 \\ -\frac{x_0\omega_1}{2} & -\frac{x_0\omega_2}{\Delta t} & 0 \\ rs\omega_1 + rsx_0\omega_3 & rs\omega_2 & -rsx_0\omega_1 \end{bmatrix}, \\
\tilde{A}_2 &= \frac{1}{\omega_1^2 + \omega_2^2 + \omega_3^2} \begin{bmatrix} 0 & 0 & \omega_2 \\ -\frac{x_0\omega_1}{2} & -\frac{x_0\omega_2}{\Delta t} & 0 \\ rs\omega_1 + rsx_0\omega_3 & rs\omega_2 & -rsx_0\omega_1 \end{bmatrix}, \\
\tilde{b}_1 &= \frac{1}{\omega_1^2 + \omega_2^2 + \omega_3^2} \begin{bmatrix} \frac{-3ax_0^2 + 2b_{\max}x_0 - fz_0/x_0 + I_{\max}}{\Delta t} \\ \frac{-cx_0\omega_2}{2} \\ rsx_0\omega_1\hat{x}_3 - rs\hat{x}_1x_0\omega_3 + \frac{cx_0^2}{2}\omega_2 \end{bmatrix}, \\
\tilde{b}_2 &= \frac{1}{\omega_1^2 + \omega_2^2 + \omega_3^2} \begin{bmatrix} \frac{-3ax_0^2 + 2b_{\min}x_0 - fz_0/x_0 + I_{\min}}{\Delta t} \\ -\frac{cx_0\omega_2}{2} \\ rsx_0\omega_1\hat{x}_3 - rs\hat{x}_1x_0\omega_3 + \frac{cx_0^2}{2}\omega_2 \end{bmatrix},
\end{aligned} \tag{4.6}$$

thus, the mapping $y = f(x) = T(x - \hat{x})$ change system (4.5) into the following system

$$\dot{y} = \begin{cases} \tilde{f}^-(y) = \tilde{A}_1 y + \tilde{b}_1 & \text{if} \quad y_1 < 0, \\ \tilde{f}^+(y) = \tilde{A}_2 y + \tilde{b}_2 & \text{if} \quad y_1 > 0. \end{cases} \tag{4.7}$$

In the subsequent numerical simulation, we consider taking $\omega^T = (1, 0, 0)$.

The neuronal system can exist in various states, such as the resting state characterized by stable membrane potential and no action potential firing, the spiking state where the membrane potential rapidly rises at a threshold followed by a quick fall, triggering an action potential in a period, the bursting state involving the firing of multiple action potentials within one period, and the chaotic state where the membrane potential displays irregular and complex fluctuations, potentially arising from intricate neuron-to-neuron interactions [32–34, 38, 39]. Without considering the control strategy, the phase plot and time series plot of system (4.1) as shown in Figure 1, if the parameters are fixed as $a = 1, b = 3, c = 6, d = 5, f = 1, r = 0.009, s = 3.966, I = 2, x_0 = -1.6$, and initial conditions $(x(0), y(0), z(0)) = (-1.5, 0.5, 0.1)$, where subfigure *a*) is the phase plot of x and y, and subfigure *b*) is the corresponding time series plot of x. According to the time series plot of the membrane potential in Figure 1, the membrane potential exhibits a quasi-periodic state. However, when the control switching threshold is set at $c_0 = 1$, $b_{max} = 3, I_{max} = 2, b_{min} = 2.5, I_{min} = 1$, and the other parameters are as same as Figure 1, It can be seen from Figure 2 that the system is in a non-periodic irregular state and the membrane potential oscillates around the switching threshold. Therefore, the decision to adopt or abandon control strategies can significantly impact the state of the system.

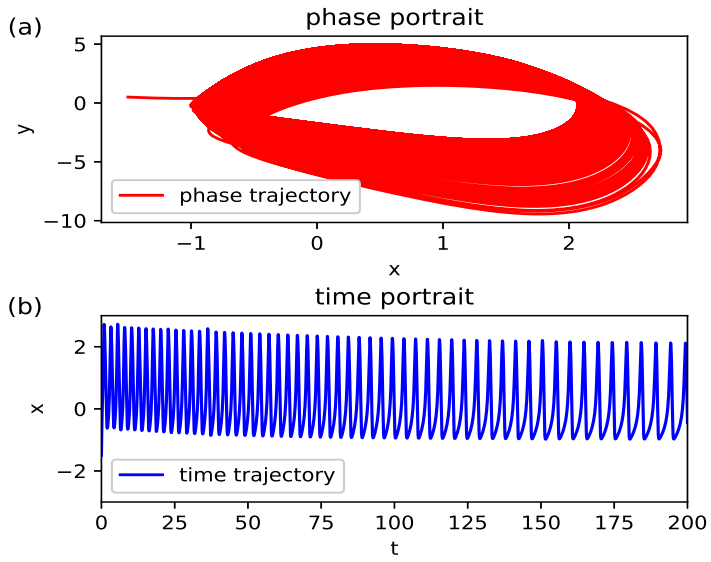

Figure 1. (a) The phase portrait of system (4.1) without control policy and (b) the time portrait of system (4.1) without control policy, the time series waveform approaches a quasi-periodic state. The parameters are set at $a = 1, b = 3, c = 6, d = 5, f = 1, r = 0.009, s = 3.966, I = 2, x_0 = -1.6$, the initial value $(x(0), y(0), z(0)) = (-1.5, 0.5, 0.1)$.

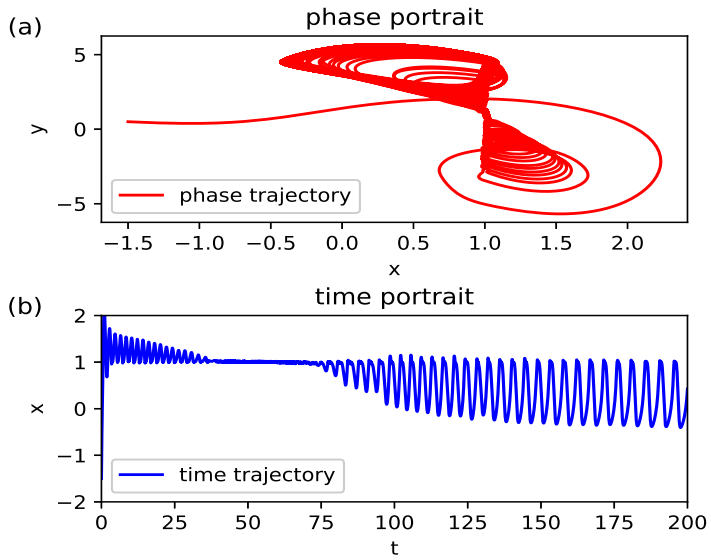

Figure 2. (a) The phase portrait of system (4.1) with control policy (4.2) and (b) the time portrait of system (4.1) with control policy (4.2). The system is in a non-periodic irregular state and the membrane potential oscillates around the switching threshold 1. The parameters are set at $a = 1, c = 6, d = 5, f = 1, r = 0.009, s = 3.966, b_{max} = 3, I_{max} = 2, b_{min} = 2.5, I_{min} = 1, x_0 = -1.6, c_0 = 1$, the initial value $(x(0), y(0), z(0)) = (-1.5, 0.5, 0.1)$.

Supposing the system parameters have been modified as $a = 1, c = 1, d = 2, f = 1, r = 0.002, s = 4$, $b_{max} = 4, I_{max} = 1, b_{min} = 1, I_{min} = 0.5, x_0 = -1.6, c_0 = 3$, and initial conditions $(x(0), y(0), z(0)) = (-1.6, 1, 0)$, then the system's phase diagram displays a limit cycle curve in Figure 3, while the corresponding time series graph of membrane potential shows spiking discharge states, with one action potential fired in a period. However, the limit cycles of Filippov systems differ from the ones of ODE, because the switching threshold c_0 alters the system's trajectory, resulting in a jagged shape for the irregular limit cycle. The firing peak of action potentials in the time series graph may be truncated due to the switching threshold c_0. Beyond spiking, bursting is another prevalent firing phenomenon in neuronal systems. When the parameters are adjusted to $a = 1, c = 4, d = 6, f = 2, r = 0.01, s = 4$, with $b_{max} = 3, I_{max} = 1, b_{min} = 1, I_{min} = 0.5$, and initial conditions $(x(0), y(0)$,z(0))=(-1.6, 1, 0), and $x_0 = -1.6, c_0 = 1.5$, the system exhibits bursting behavior, characterized by multiple action potentials fired within a single period. The corresponding phase diagram with transient state and time series plot are shown in Figure 4. Similarly, the firing peak of bursting is influenced by the switching threshold. If the firing peak exceeds the threshold, the system trajectory will contract towards the direction below the switching threshold due to the switching effect of the Filippov system. The crossing limit cycle implies that the trajectory of the limit cycle passes through the switching line (or plane), spanning at least two subsystems. In neuronal systems, a limit cycle in the phase portrait implies that the corresponding membrane potential state variable of neurons are in a periodic spiking state.

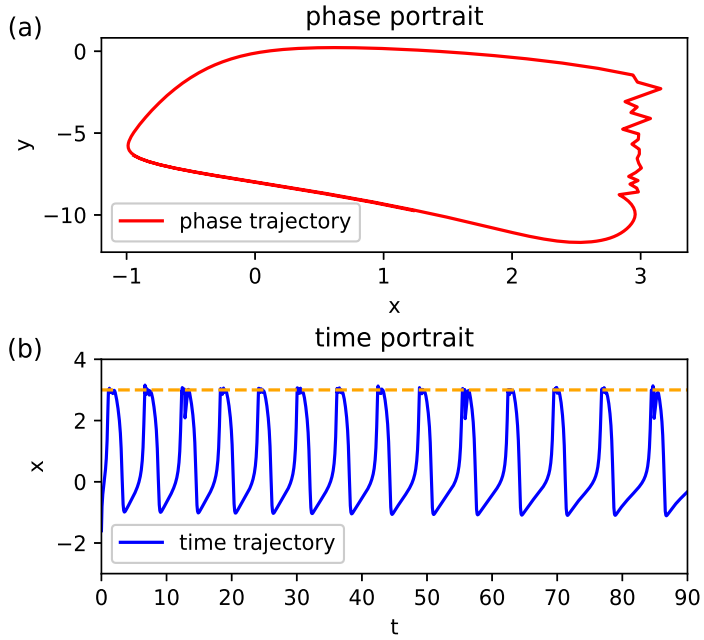

Figure 3. (a) The phase portrait of system (4.1) with control policy (4.2) and (b) the time portrait of system (4.1) with control policy (4.2). The phase portrait exhibits irregular limit cycles, while the time series plot shows spiking phenomena. The parameters are set at $a = 1, c = 1, d = 2, f = 1, r = 0.002, s = 4, b_{max} = 4, I_{max} = 1, b_{min} = 1, I_{min} = 0.5, x_0 = -1.6, c_0 = 3$, the initial value $(x(0), y(0), z(0)) = (-1.6, 1, 0)$.

If the values of the other parameters are fixed as shown in Figure 4, and the switching threshold is adjusted to $c_0 = 0.7$, the resulting Poincare section at $x = 0$ of the scatter plot in the $y - z$ plane, as shown in Figure 5. The scatter plot contains four fixed points, indicating the coexistence of multiple attractors in the system. Additionally, Figure 6 shows the corresponding three-dimensional Poincare section with the same parameters as Figure 5. The periodic solutions appear as four closed orbits in a three-dimensional space, contrasted with the four fixed points observed in the two-dimensional plane. The coexistence of multiple attractors refers to the existence of multiple attractors that can attract the system state towards different stable states or periodic orbits. This phenomenon indicates that the system has multiple stable states, and transitions or mutual influences may exist among these states. Note that Figures 4–6, where the switching threshold values differ (Figure 4: $c_0 = 1.5$, Figures 5 and 6: $c_0 = 0.7$) while the remaining parameter values are the same, the system's dynamical behavior is completely different. Figure 4 exhibits a single stable state, whereas Figures 5 and 6 depict multiple stable states. The switching threshold can cause the system to switch between different states and greatly alter the system's state.

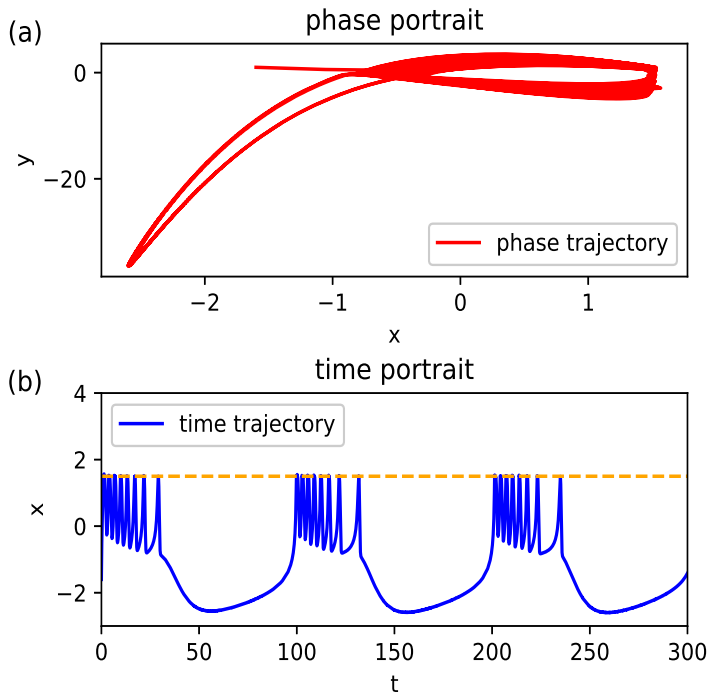

Figure 4. (a) The phase portrait of system (4.1) with control policy (4.2) and (b) the time portrait of system (4.1) with control policy (4.2). The phase portrait represents limit cycles (with transient state preserved), while the time series plot shows bursting phenomena. The parameters are set at $a = 1, c = 4, d = 6, f = 2, r = 0.01, s = 4, b_{max} = 3, I_{max} = 1, b_{min} = 1, I_{min} = 0.5, x_0 = -1.6, c_0 = 1.5$, the initial value $(x(0), y(0), z(0)) = (-1.6, 1, 0)$.

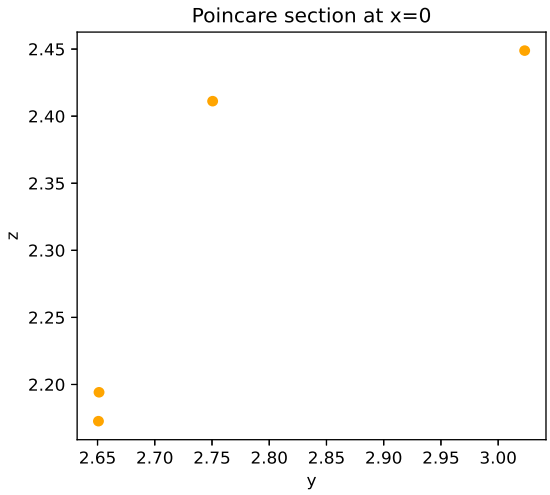

Figure 5. The 2D Poincare section of system (4.1) with control policy (4.2). The four dots in the figure indicate the coexistence of four attractors in the system. The parameters are set at $a = 1, c = 4, d = 6, f = 2, r = 0.01, s = 4, b_{max} = 3, I_{max} = 1, b_{min} = 1, I_{min} = 0.5, x_0 = -1.6, c_0 = 0.7$, the initial value $(x(0), y(0), z(0)) = (-1.6, 1, 0)$.

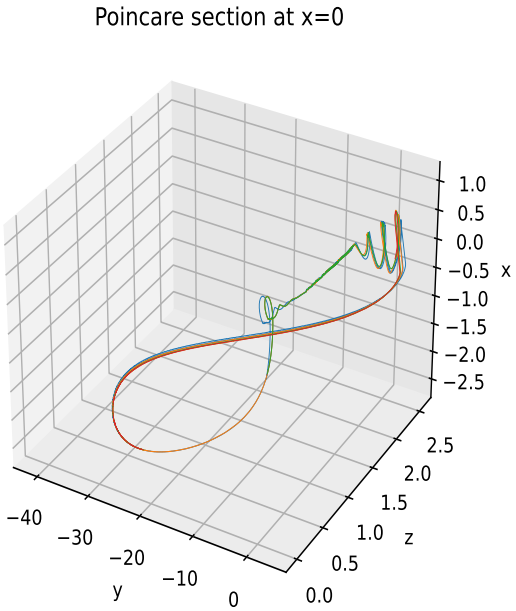

Figure 6. The 3D Poincare section of system (4.1) with control policy (4.2). The four closed curves in the figure indicate the coexistence of four limit cycles in the system. The parameters are set at $a = 1, c = 4, d = 6, f = 2, r = 0.01, s = 4, b_{max} = 3, I_{max} = 1, b_{min} = 1, I_{min} = 0.5, x_0 = -1.6, c_0 = 0.7$, the initial value $(x(0), y(0), z(0)) = (-1.6, 1, 0)$.

The parameter b is another key parameter that influences the dynamical behavior of the Hindmarsh-Rose neuron system. b serves as the bifurcation parameter, and three bifurcation diagrams are used to illustrate the trends of the state variables as b changes within a certain range. Figure 7 illustrates the bifurcation diagram on the $b - x$ plane, revealing a period-doubling bifurcation phenomenon occurring for the values of b between around 5 and 6. When there are two membrane potential values for the same parameter value b, it indicates that the system is in a bistable state. This means that the system can simultaneously exist in two stable states, each with a different membrane potential value. The system can switch between these two states, and within the given parameter range, this switching is reversible. This phenomenon is common in dynamical systems and indicates that the system can exhibit multiple stable patterns under specific conditions. Likewise, when there are four distinct membrane potential values for the same parameter value b, it indicates the system entering a multistable state. This implies that the system can exist in four stable states simultaneously, each characterized by a different membrane potential value, with the ability to switch between them. Figures 8 and 9 depict the bifurcation diagrams on the $b - y$ plane and $b - z$ plane, respectively, for the same parameters as in Figure 7. The bifurcation phenomenon on the $b - y$ plane exhibits similarities with the bifurcation pattern observed on the $b - x$ plane, period-doubling bifurcation emerges near 5 to 6 for b. However, the bifurcation patterns on the $b - z$ plane are less pronounced. At b values around 5 and 6, there is no bifurcation phenomenon, but the rate of increase in the z value becomes accelerated. This could be attributed to the fact that y is a fast variable, while z is a slow variable. The role of the recovery variable y is more significant, while the regulatory effect of the slow variable z is limited.

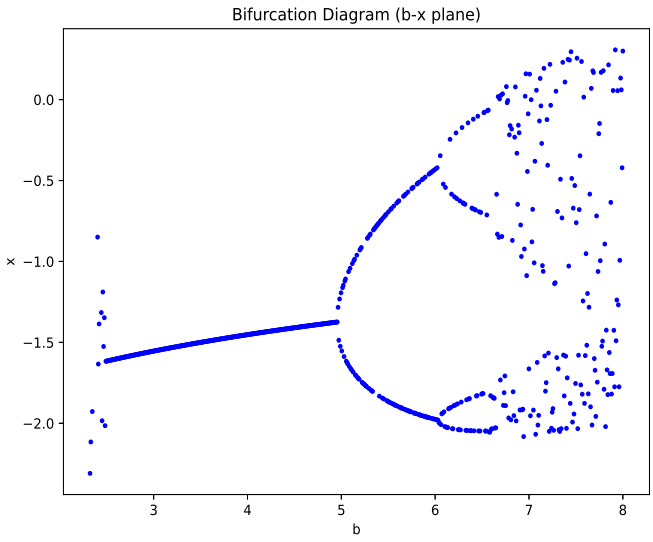

Figure 7. The bifurcation diagram of system (4.1) with control policy (4.2) on $b - x$ plane. The system exhibits period-doubling bifurcations, transitioning from a single period to double period, and then to quadruple period. The parameters are set at $a = 1, c = 1, d = 5, f = 5, r = 0.009, s = 4, b_{max} \in [0, 8], I_{max} = 1, b_{min} = 0.25b_{max}, I_{min} = 0.5, x_0 = -1.6, c_0 = 1$, the initial value $(x(0), y(0), z(0)) = (-1.6, 0.5, 0.1)$.

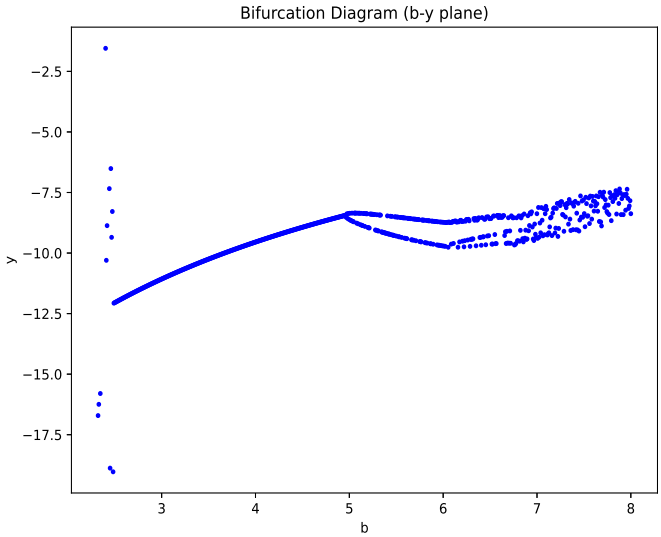

Figure 8. The bifurcation diagram of system (4.1) with control policy (4.2) on $b - y$ plane. The system exhibits period-doubling bifurcations, transitioning from a single period to double period. The parameters are set at $a = 1, c = 1, d = 5, f = 5, r = 0.009, s = 4, b_{max} \in [0, 8], I_{max} = 1, b_{min} = 0.25b_{max}, I_{min} = 0.5, x_0 = -1.6, c_0 = 1$, the initial value $(x(0), y(0), z(0)) = (-1.6, 0.5, 0.1)$.

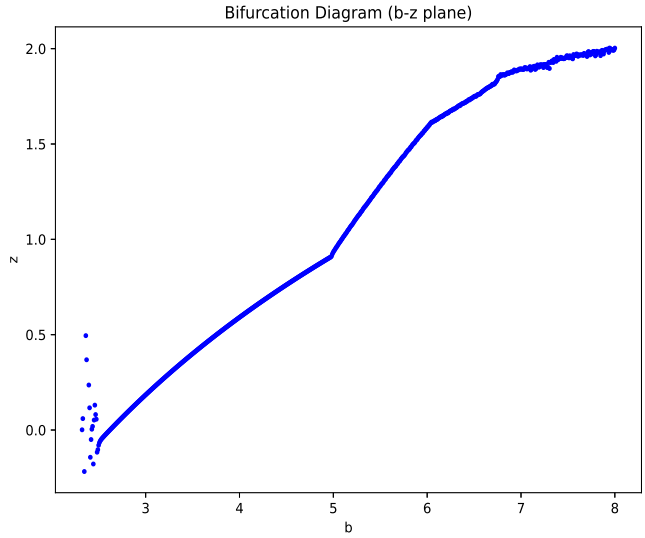

Figure 9. The bifurcation diagram of system (4.1) with control policy (4.2) on $b - z$ plane. The variable z is directly proportional to the parameter b. The parameters are set at $a = 1, c = 1, d = 5, f = 5, r = 0.009, s = 4, b_{max} \in [0, 8], I_{max} = 1, b_{min} = 0.25b_{max}, I_{min} = 0.5, x_0 = -1.6, c_0 = 1$, the initial value $(x(0), y(0), z(0)) = (-1.6, 0.5, 0.1)$.

5. Summary and conclusions

In this paper, we study the pseudo-Hopf bifurcation in Filippov Hindmarsh-Rose neuron system, the existence of crossing limit cycles is proved by constructing half-return mapping. While research on crossing limit cycles have primarily focused on linear systems, we expand the analysis to nonlinear neuronal system. The trajectory of crossing limit cycle in Filippov neuron systems differs from that in ordinary differential equations (ODEs) mainly in the sense that its trajectory crosses discontinuous boundaries and is distributed in two or more subsystems. The periodic firing phenomenon of membrane potential (spiking or bursting) is altered or truncated due to the threshold switching, which means changes in the threshold can alter or even cut off the waveform of action potential of a neuron.

Neuronal systems are inherently complex, exhibiting a diverse range of firing patterns, and threshold control further alters the system's firing states. By implementing threshold control, it becomes possible to switch the system's firing state, such as transitioning from a non-periodic state to a periodic state or evolving from spiking to bursting. Additionally, the system exhibits the coexistence of multiple attractors and period-doubling bifurcation through threshold control. Within specific ranges of parameter values, the system can generate multiple stable states, allowing for the membrane potential to transition among these states. In period-doubling bifurcation, as the system parameter changes, the system transitions from stable periodic behavior to increasingly complex periodic behavior. Eventually, as the bifurcation progresses, the system enters a highly sensitive to initial conditions, seemingly random, and unpredictable chaotic state. We focus on neuronal systems, and in the future, we will explore various threshold control strategies for network nodes, as well as the implications of multiple thresholds on neural networks.

Author contributions

Yi Yang: Funding acquisition, Writing-original draft, Conceptualization, Formal analysis, Methodology; Rongfeng Li: Supervision, Writing-review and editing; Xiangguang Dai: Funding acquisition, Validation and data analysis, Supervision; Haiqing Li: Writing-review, and editing; Changcheng Xiang: Funding acquisition, Software, Methodology. All authors have read and approved the final version of the manuscript for publication.

Use of AI tools declaration

The authors declare they have not used Artificial Intelligence (AI) tools in the creation of this article.

Acknowledgments

This work was supported in part by the National Natural Science Foundation of China (Grant No.12201086, 12361100), this work was also supported in part by the Chongqing Education Commission Youth Project (Grant No. KJQN202201209, KJQN202301245). The work was also supported by the Science and Technology Research Program of Chongqing Municipal Education Commission (Grant No. KJZD-M202201204, KJZD-K202201205).

Conflict of interest

The authors declare no conflict of interest.

References

1. B. D. Hassard, N. D. Kazarinoff, Y. H. Wan, *Theory and applications of Hopf bifurcation*, Cambridge University Press, 1981. https://archive.org/details/theoryapplicatio0000hass
2. J. Guckenheimer, P. Holmes, *Nonlinear oscillations, dynamical systems, and bifurcations of vector fields*, Springer, 1984. https://doi.org/10.1115/1.3167759
3. S. H. Strogatz, *Nonlinear dynamics and Chaos: With applications to physics, biology, chemistry, and engineering*, 2 Eds., CRC Press, 2018. https://doi.org/10.1201/9780429492563
4. Y. A. Kuznetsov, *Elements of applied bifurcation theory*, 2 Eds., Springer, 1998. Availble from: `https://link.springer.com/book/10.1007/978-1-4757-3978-7`.
5. A. Filippov, *Differential equations with discontinuous right-hand sides*, Kluwer Academic Publishers, 1988. https://doi.org/10.1007/978-94-015-7793-9
6. Y. A. Kuznetsov, S. Rinaldi, A. Gragnani, One parameter bifurcations in planar filippov systems, *Int. J. Bifurcat. Chaos*, **13** (2003), 2157–2188. https://doi.org/10.1142/S0218127403007874
7. E. Freire, E. Ponce, F. Torres, On the critical crossing cycle bifurcation in planar filippov systems, *J. Differ. Equations*, **259** (2015), 7086–7107. https://doi.org/10.1016/j.jde.2015.08.013
8. Y. Yang, X. Liao, Filippov hindmarsh-rose neuronal model with threshold policy control, *IEEE T. Neur. Net. Lear.*, **30** (2018), 306–311. https://doi.org/10.1109/TNNLS.2018.2836386
9. H. Zhou, S. Tang, Bifurcation dynamics on the sliding vector field of a filippov ecological system, *Appl. Math. Comput.*, **424** (2022), 127052. https://doi.org/10.1016/j.amc.2022.127052
10. J. Castillo, J. Llibre, F. Verduzco, The pseudo-hopf bifurcation for planar discontinuous piecewise linear differential systems, *Nonlinear Dyn.*, **90** (2017), 1829–1840. https://doi.org/10.1007/s11071-017-3766-9
11. J. M. Islas, J. Castillo, B. Aguirre-Hernandez, F. Verduzco, Pseudo-hopf bifurcation for a class of 3d filippov linear systems, *Int. J. Bifurcat. Chaos*, **31** (2021), 2150025. https://doi.org/10.1142/S0218127421500255
12. D. D. Novaes, L. A. Silva, On the cyclicity of monodromic tangential singularities: A look beyond the pseudo-hopf bifurcation, *J. Nonlinear Sci.*, **33** (2023), 189–215. https://doi.org/10.48550/arXiv.2303.06027
13. J. Castillo, The pseudo-hopf bifurcation and derived attractors in 3d filippov linear systems with a teixeira singularity, *Chaos*, **30** (2020), 113101. https://doi.org/10.1063/5.0014830
14. L. Li, Three crossing limit cycles in planar piecewise linear systems with saddle-focus type, *Electron. J. Qual. Theo.*, **2014** (2014), 1–14. https://doi.org/10.14232/ejqtde.2014.1.70
15. E. Ponce, J. Ros, E. Vela, The boundary focus-saddle bifurcation in planar piecewise linear systems. application to the analysis of memristor oscillators, *Nonlinear Anal. Real World Appl.*, **43** (2018), 495–514. https://doi.org/10.1016/j.nonrwa.2018.03.011

16. J. Wang, C. Huang, L. Huang, Discontinuity-induced limit cycles in a general planar piecewise linear system of saddle-focus type, *Nonlinear Anal. Hybrid Syst.*, **33** (2019), 162–178. https://doi.org/10.1016/j.nahs.2019.03.004
17. S.-M. Huan, X.-S. Yang, Existence of limit cycles in general planar piecewise linear systems of saddle-saddle dynamics, *Nonlinear Anal.*, **92** (2013), 82–95. https://doi.org/10.1016/j.na.2013.06.017 Get rights and content
18. S. M. Huan, X. S. Yang, On the number of limit cycles in general planar piecewise linear systems of node-node types, *J. Math. Anal. Appl.*, **411** (2014), 340–353. https://doi.org/10.1016/j.jmaa.2013.08.064
19. J. Wang, X. Chen, L. Huang, The number and stability of limit cycles for planar piecewise linear systems of node-saddle type, *J. Math. Anal. Appl.*, **469** (2019), 405–427. https://doi.org/10.1016/j.jmaa.2018.09.024
20. J. Llibre, E. Ponce, F. Torres, On the existence and uniqueness of limit cycles in liénard differential equations allowing discontinuities, *Nonlinearity*, **21** (2008), 2121–2142. https://doi.org/10.1088/0951-7715/21/9/013
21. E. Freire, E. Ponce, F. Torres, Canonical discontinuous planar piecewise linear systems, *SIAM J. Appl. Dyn. Syst.*, **11** (2012), 181–211. https://doi.org/10.1137/11083928X
22. F. Jiang, M. Han, Qualitative analysis of crossing limit cycles in discontinuous liénard-type differential systems, *J. Nonlinear Model. Anal.*, **1** (2019), 527–543. https://doi.org/10.12150/jnma.2019.527
23. R. Cristiano, D. Pagano, T. Carvalho, D. J. Tonon, Bifurcations at a degenerate two-fold singularity and crossing limit cycles, *J. Differ. Equations*, **268** (2019), 115–140. https://doi.org/10.1016/j.jde.2019.08.024
24. L. F. Gouveia, J. Torregrosa, 24 crossing limit cycles in only one nest for piecewise cubic systems, *Appl. Math. Lett.*, **103** (2020), 106189. https://doi.org/10.1016/j.aml.2019.106189
25. J. L. Cardoso, J. Llibre, D. D. Novaes, D. J. Tonon, Simultaneous occurrence of sliding and crossing limit cycles in piecewise linear planar vector fields, *Dyn. Syst.*, **2020** (2020), 1722064. https://doi.org/10.1080/14689367.2020.1722064
26. R. Benterki, J. Llibre, Crossing limit cycles of planar piecewise linear hamiltonian systems without equilibrium points, *Mathematics*, **8** (2020), 8050755. https://doi.org/10.3390/math8050755
27. Z. Jin, Crossing limit cycles of planar piecewise hamiltonian systems with linear centers separated by two parallel straight lines, *J. Appl. Math. Phys.*, **11** (2023), 1429–1447. https://doi.org/10.4236/jamp.2023.115093
28. M. Colombo, E. di Bernardo, E. Fossas, M. Jeffrey, Teixeira singularities in 3d switched feedback control systems, *Syst. Control Lett.*, **59** (2010), 615–622. https://doi.org/10.1016/j.sysconle.2010.07.006
29. A. Colombo, M. R. Jeffrey, Nondeterministic chaos, and the two-fold singularity in piecewise smooth flows, *SIAM J. Appl. Dyn. Syst.*, **10** (2011), 423–451. https://doi.org/10.1137/100801846

30. R. Cristiano, E. Ponce, D. J. Pagano, M. Granzotto, On the teixeira singularity bifurcation in a dc–dc power electronic converter, *Nonlinear Dyn.*, **96** (2019), 1243–1266. https://doi.org/10.1007/s11071-019-04851-8

31. R. Cristiano, D. J. Pagano, E. Freire, E. Ponce, Revisiting the teixeira singularity bifurcation analysis: Application to the control of power converters, *Int. J. Bifurcat. Chaos*, **28** (2018), 1850106. https://doi.org/10.1142/S0218127418501067

32. H. Bao, A. Hu, W. Liu, B. Bao, Hidden bursting firings and bifurcation mechanisms in memristive neuron model with threshold electromagnetic induction, *IEEE Trans. Neural Netw. Learn. Syst.*, **31** (2020), 502–511. https://doi.org/10.1109/TNNLS.2019.2905137

33. Z. Tabekoueng Njitacke, J. Kengne, H. B. Fotsin, Coexistence of multiple stable states and bursting oscillations in a 4d hopfield neural network, *Circuits Syst. Signal Process.*, **39** (2020), 3424–3444. https://doi.org/10.1007/s00034-019-01324-6

34. H. Lin, C. Wang, C. Chen, Y. Sun, C. Zhou, C. Xu, Q. Hong, Neural bursting and synchronization emulated by neural networks and circuits, *IEEE Trans. Circuits Syst. I*, **68** (2021), 3397–3410. https://doi.org/10.1109/TCSI.2021.3081150

35. Y. Li, Z. Wei, T. Kapitaniak, W. Zhang, Stochastic bifurcation and chaos analysis for a class of ships rolling motion under non-smooth perturbation and random excitation, *Ocean Eng.*, **266** (2022), 112859. https://doi.org/10.1016/j.oceaneng.2022.112859

36. Y. Wu, L. Wu, Y. Zhu, M. Yi, L. Lu, Enhancing weak signal propagation by intra- and inter-layer global couplings in a feedforward network, *Chaos Soliton. Fract.*, **181** (2024), 114566. https://doi.org/10.1016/j.chaos.2024.114566

37. J. L. Hindmarsh, R. M. Rose, A model of neuronal bursting using three coupled first order differential equations, *P. Roy. Soc. Lond. B.*, **221** (1984), 87–102. https://doi.org/10.1098/rspb.1984.0024

38. E. M. Izhikevich, Neural excitability, spiking and bursting, *Int. J. Bifurcat. Chaos*, **10** (2000), 1171–1266. https://doi.org/10.1142/S0218127400000840

39. E. M. Izhikevich, Which model to use for cortical spiking neurons? *IEEE Trans. Neural Netw.*, **15** (2004), 1063–1070. https://doi.org/10.1109/TNN.2004.832719

Appendix: The half-return maps

To establish the existence of a crossing limit cycle, we need to identify vectors $q_1 = \begin{pmatrix} 0 \\ u_1 \\ v_1 \end{pmatrix}$ and $q_2 = \begin{pmatrix} 0 \\ u_2 \\ v_2 \end{pmatrix}$, where $u_1, v_1 < 0$ and $u_2, v_2 > 0$. Furthermore, we should determine the corresponding times t_1, t_2 such that the system

$$q_2 = \varphi^-_{t_1}(q_1), \tag{5.1a}$$

$$q_1 = \varphi^+_{t_2}(q_2), \tag{5.1b}$$

has a solution, where $\varphi_{t_1}^{-}(q_1)$ is defined as

$$\varphi_{t_1}^{-}(q_1) = e^{t_1\tilde{A}_1}\left(q_1 + \int_0^{t_1} e^{-s\tilde{A}_1}\tilde{b}_1 ds\right). \tag{5.2}$$

Additionally, according to the properties of the exponential matrix, we can state that

$$e^{-s\tilde{A}_1} = I - s\tilde{A}_1 + \frac{s^2}{2!}\tilde{A}_1^2 - \frac{s^3}{3!}\tilde{A}_1^3 + \cdots$$

$$e^{t_1\tilde{A}_1} = I + t_1\tilde{A}_1 + \frac{t_1^2}{2!}\tilde{A}_1^2 + \frac{t_1^3}{3!}\tilde{A}_1^3 + \cdots$$

thus,

$$\begin{aligned}\int_0^{t_1} e^{-s\tilde{A}_1}\tilde{b}_1 ds &= \int_0^{t_1}\left[I - s\tilde{A}_1 + \frac{s^2}{2!}\tilde{A}_1^2 - \frac{s^3}{3!}\tilde{A}_1^3 + \cdots\right]\tilde{b}_1 ds = \int_0^{t_1}\left[\tilde{b}_1 - s\tilde{A}_1\tilde{b}_1 + \frac{s^2}{2!}\tilde{A}_1^2\tilde{b}_1 - \frac{s^3}{3!}\tilde{A}_1^3\tilde{b}_1 + \cdots\right]ds \\ &= \tilde{b}_1 t_1 - \frac{1}{2}\tilde{A}_1\tilde{b}_1 t_1^2 + \frac{1}{2!}\cdot\frac{1}{3}t_1^3\tilde{A}_1^2\tilde{b}_1 - \frac{1}{3!}\cdot\frac{1}{4}t_1^4\tilde{A}_1^3\tilde{b}_1 + \ldots\end{aligned}$$

and

$$\begin{aligned}e^{t_1\tilde{A}_1}\left(q_1 + \int_0^{t_1} e^{-s\tilde{A}_1}\tilde{b}_1 ds\right) &= \left[I + t_1\tilde{A}_1 + \frac{t_1^2}{2!}\tilde{A}_1^2 + \frac{t_1^3}{3!}\tilde{A}_1^3 + \cdots\right]\times\left[q_1 + \tilde{b}_1 t_1 - \frac{1}{2!}\tilde{A}_1\tilde{b}_1 t_1^2 + \frac{1}{3!}t_1^3\tilde{A}_1^2\tilde{b}_1 - \frac{1}{4!}t_1^4\tilde{A}_1^3\tilde{b}_1 + \cdots\right] \\ &= q_1 + \tilde{b}_1 t_1 - \frac{1}{2!}\tilde{A}_1\tilde{b}_1 t_1^2 + \frac{1}{3!}\tilde{A}_1^2\tilde{b}_1 t_1^3 - \frac{1}{4!}\tilde{A}_1^3\tilde{b}_1 t_1^4 + \tilde{A}_1 q_1 t_1 + \tilde{A}_1\tilde{b}_1 t_1^2 - \frac{1}{2!}\tilde{A}_1^2\tilde{b}_1 t_1^3 \\ &\quad + \frac{1}{3!}\tilde{A}_1^3\tilde{b}_1 t_1^4 - \frac{1}{4!}\tilde{A}_1^4\tilde{b}_1 t_1^5 + \frac{1}{2!}\tilde{A}_1^2 q_1 t_1^2 + \frac{\widetilde{A_1^2}}{2!}\tilde{b}_1 t_1^3 - \frac{\tilde{A}_1^3}{2!2!}\tilde{b}_1 t_1^4 + \frac{\tilde{A}_1^4}{2!3!}\tilde{b}_1 t_1^5 - \frac{\tilde{A}_1^5}{2!4!}\tilde{b}_1 t_1^6 \\ &\quad + \frac{\tilde{A}_1^3}{3!}q_1 t_1^3 + \frac{\tilde{A}_1^3}{3!}\tilde{b}_1 t_1^4 - \frac{\tilde{A}_1^4}{3!2!}\tilde{b}_1 t_1^5 + \frac{\tilde{A}_1^5}{3!3!}\tilde{b}_1 t_1^6 - \frac{\tilde{A}_1^6}{3!4!}\tilde{b}_1 t_1^7 + \cdots\end{aligned}$$

therefore, the mapping (5.1a) can be rewritten as the following

$$q_2 = q_1 + t_1 N_1(t_1)\,\tilde{g}(q_1), \tag{5.3}$$

the equation is equivalent to

$$\begin{pmatrix} 0 \\ u_2 \\ v_2 \end{pmatrix} = \begin{pmatrix} 0 \\ u_1 \\ v_1 \end{pmatrix} + \begin{pmatrix} t_1 e_1^T N_1(t_1)\tilde{g}(q_1) \\ t_1 e_2^T N_1(t_1)\,\tilde{g}(q_1) \\ t_1 e_3^T N_1(t_1)\,\tilde{g}(q_1) \end{pmatrix}, \tag{5.4}$$

where

$$N_1(t_1) = I + \frac{t_1}{2!}\tilde{A}_1 + \frac{t_1^2}{3!}\tilde{A}_1^2 + \frac{t_1^3}{4!}\tilde{A}_1^3 + \cdots$$

thus,

$$\begin{aligned}q_1 + t_1 N_1(t_1)\,\tilde{g}^{-}(q_1) =& q_1 + \left[t_1 + \frac{t_1^2}{2!}\tilde{A}_1 + \frac{t_1^3}{3!}\tilde{A}_1^2 + \frac{t_1^4}{4!}\tilde{A}_1^3 + \cdots\right]\left[\tilde{A}_1 q_1 + \tilde{b}_1\right] \\ =& q_1 + \tilde{b}_1 t_1 + \frac{t_1^2}{2!}\tilde{A}_1\tilde{b}_1 + \frac{t_1^3}{3!}\tilde{A}_1^2\tilde{b}_1 + \frac{t_1^4}{4!}\tilde{A}_1^3\tilde{b}_1 + \tilde{A}_1 q_1 t_1 + \frac{t_1^2}{2!}\tilde{A}_1^2 q_1 \\ &+ \frac{t_1^3}{3!}\tilde{A}_1^3 q_1 + \frac{t_1^4}{4!}\tilde{A}_1^4 q_1 + \frac{t_1^5}{5!}\tilde{A}_1^5 q_1 + \frac{t_1^5}{5!}\tilde{A}_1^4\tilde{b}_1 + \cdots\end{aligned}$$

by comparing it's obvious that

$$e^{t_1\tilde{A}_1}\left(q_1+\int_0^{t_1}e^{-s\tilde{A}_1}\tilde{b}_1ds\right)=q_1+t_1N_1\left(t_1\right)\tilde{g}\left(q_1\right).$$

According to the first equation of (5.4),

$$t_1e_1^TN_1\left(t_1\right)\tilde{g}^-\left(q_1\right)=0, \tag{5.5}$$

that is

$$\begin{aligned}
G_1\left(t_1,u_1,v_1\right)&=e_1^TN_1\left(t_1\right)\tilde{g}^-\left(q_1\right)\\
&=\begin{pmatrix}1&0&0\end{pmatrix}\left[I+\frac{t_1}{2!}\tilde{A}_1+\frac{t_1^2}{3!}\tilde{A}_1^2+\frac{t_1^3}{4!}\tilde{A}_1^3+\cdots\right]\times\left[\tilde{A}_1\left(q_1\right)+\tilde{b}_1\right]\\
&=\begin{pmatrix}1&0&0\end{pmatrix}\left[\begin{pmatrix}1&0&0\\0&1&0\\0&0&1\end{pmatrix}+\frac{t_1}{2!}\begin{pmatrix}0&1&0\\c_1&c_2&c_3\\c_4&c_5&c_6\end{pmatrix}\right.\\
&\quad\left.+\frac{t_1^2}{3!}\begin{pmatrix}c_1&c_2&c_3\\c_1c_2+c_3c_4&c_1+c_2^2+c_3c_5&c_2c_3+c_3c_6\\c_1c_5+c_4c_6&c_4+c_2c_5+c_5c_6&c_3c_5+c_6^2\end{pmatrix}+\cdots\right]\times\left[\begin{pmatrix}0&1&0\\c_1&c_2&c_3\\c_4&c_5&c_6\end{pmatrix}\begin{pmatrix}0\\u_1\\v_1\end{pmatrix}+\begin{pmatrix}0\\r_1\\s_\mu\end{pmatrix}\right]\\
&=\left[\begin{pmatrix}1&0&0\end{pmatrix}+\frac{t_1}{2!}\begin{pmatrix}0&1&0\end{pmatrix}+\frac{t_1^2}{3!}\begin{pmatrix}c_1&c_2&c_3\end{pmatrix}+\cdots\right]\times\left[\begin{pmatrix}u_1\\c_2u_1+c_3v_1\\c_5u_1+c_6v_1\end{pmatrix}+\begin{pmatrix}0\\r_1\\s_\mu\end{pmatrix}\right]\\
&=u_1+\frac{t_1}{2}\left(r_1+c_2u_1+c_3v_1\right)+\frac{t_1^2}{6}\left[c_1u_1+c_2\left(c_2u_1+c_3v_1+r_1\right)+c_3\left(c_5u_1+c_6v_1+s_\mu\right)\right]+\cdots\\
&=u_1+\frac{t_1}{2}\left(r_1+c_2u_1+c_3v_1\right)+\frac{t_1^2}{6}\eta_1+\cdots
\end{aligned} \tag{5.6}$$

where $\eta_1=c_2r_1+c_3s_\mu+\left(c_1+c_3c_5+c_2^2\right)u_1+c_3\left(c_2+c_6\right)v_1$, $s_\mu=s_1+\mu$. Simple calculation shows that $G_1\left(0,0,0\right)=0$ and $\frac{\partial G_1}{\partial t_1}(0,0,0)=\frac{r_1}{2}\neq 0$. Thus, by the implicit function theorem, there exists a function

$$t_1\left(u_1,v_1\right)=a_1u_1+a_2v_1+a_3u_1v_1+a_4u_1^2+a_5v_1^2+a_6u_1^2v_1+a_7u_1v_1^2+\cdots,$$

such that $G_1\left(t_1\left(u_1,v_1\right),u_1,v_1\right)\equiv 0$ in a neighborhood of $(0,0,0)$. Substituting $t_1\left(u_1,v_1\right)$ into $G_1\left(t_1,u_1,v_1\right)$, thus

$$\begin{aligned}
G_1\left(t_1\left(u_1,v_1\right),u_1,v_1\right)&=u_1+\frac{1}{2}\left(a_1u_1+a_2v_1+a_3u_1v_1+a_4u_1^2+a_5v_1^2+a_6u_1^2v_1+a_7u_1v_1^2+\cdots\right)\times\left(r_1+c_2u_1+c_3v_1\right)\\
&\quad+\frac{1}{6}\left(a_1u_1+a_2v_1+a_3u_1v_1+a_4u_1^2+a_5v_1^2+a_6u_1^2v_1+a_7u_1v_1^2+\cdots\right)^2\eta_1\\
&\equiv 0.
\end{aligned}$$

Since $G_1\left(t_1\left(u_1,v_1\right),u_1,v_1\right)\equiv 0$, we can infer that the coefficients associated with u and v are all zero. By calculation, it can be determined

$$\begin{aligned}
&a_1=-\frac{2}{r_1},\quad a_2=0,\quad a_3=\frac{2c_3}{r_1^2},\quad a_4=\frac{2\left(c_2r_1-2c_3s_u\right)}{3r_1^3},\\
&a_5=0,\quad a_6=\frac{12c_3^2s_u-4c_3\left(c_2+c_6\right)r_1}{3r_1^4},\quad a_7=\frac{-2c_3^2}{r_1^3},
\end{aligned}$$

thus, $t_1(u_1, v_1)$ is represented as

$$t_1(u_1, v_1) = -\frac{2u_1}{r_1} + \frac{2c_3u_1v_1}{r_1^2} + \frac{2\left(c_2r_1 - 2c_3s_\mu\right)u_1^2}{3r_1^3} - \frac{4c_3u_1^2v_1\left((c_2 + c_6)r_1 - 3c_3s_\mu\right)}{3r_1^4} - \frac{2c_3^2u_1v_1^2}{r_1^3} + \cdots.$$

By substituting t_1 into the second and third equations of (5.4), we obtain

$$\begin{pmatrix} u_2 \\ v_2 \end{pmatrix} = \begin{pmatrix} \varphi_{11}^-(u_1, v_1) \\ \varphi_{12}^-(u_1, v_1) \end{pmatrix} = \begin{pmatrix} u_1 + t_1(u_1, v_1)\, e_2^T N_1(t_1(u_1, v_1))\, \tilde{g}^-(q_1) \\ v_1 + t_1(u_1, v_1)\, e_3^T N_1(t_1(u_1, v_1))\, \tilde{g}^-(q_1) \end{pmatrix}. \tag{5.7}$$

Firstly, let's calculate $\varphi_{11}^-(u_1, v_1)$

$$\begin{aligned}
\varphi_{11}^-(u_1, v_1) &= u_1 + t_1(u_1, v_1)\, e_2^T N_1(t_1(u_1, v_1))\, \tilde{g}^-(q_1) \\
&= u_1 + t_1 \begin{pmatrix} 0 & 1 & 0 \end{pmatrix} \left[I + \frac{t_1}{2!}\tilde{A}_1 + \frac{t_1^2}{3!}\tilde{A}_1^2 + \cdots \right] \times \left[\tilde{A}_1 \begin{pmatrix} 0 \\ u_1 \\ v_1 \end{pmatrix} + \begin{pmatrix} 0 \\ r_1 \\ s_\mu \end{pmatrix} \right] \\
&= u_1 + \left\{ \begin{array}{l} t_1 \begin{pmatrix} 0 & 1 & 0 \end{pmatrix} + \frac{t_1^2}{2!} \begin{pmatrix} 0 & 1 & 0 \end{pmatrix} \begin{pmatrix} 0 & 1 & 0 \\ c_1 & c_2 & c_3 \\ c_4 & c_5 & c_6 \end{pmatrix} \\ \qquad + \frac{t_1^3}{3!} \begin{pmatrix} 0 & 1 & 0 \end{pmatrix} \begin{pmatrix} 0 & 1 & 0 \\ c_1 & c_2 & c_3 \\ c_4 & c_5 & c_6 \end{pmatrix}^2 + \cdots \end{array} \right\} \times \begin{bmatrix} u_1 \\ c_2u_1 + c_3v_1 + r_1 \\ c_5u_1 + c_6v_1 + s_u \end{bmatrix} \\
&= u_1 + t_1(c_2u_1 + c_3v_1 + r_1) + \frac{t_1^2}{2!}\left[c_1u_1 + c_2(c_2u_1 + c_3v_1 + r_1) + c_3\left(c_5u_1 + c_6v_1 + s_\mu\right) \right] \\
&\quad + \frac{t_1^3}{3!}\left[(c_1c_2 + c_3c_4)u_1 + (c_1 + c_2^2 + c_3c_5) \times (c_2u_1 + c_3v_1 + r_1) + (c_2c_3 + c_3c_6)(c_5u_1 + c_6v_1 + s_u) \right] \\
&\quad + \cdots \\
&= u_1 + \left[-\frac{2u_1}{r_1} + \frac{2c_3u_1v_1}{r_1^2} + \frac{2\left(c_2r_1 - 2c_3s_\mu\right)u_1^2}{3r_1^3} - \frac{2c_3^2u_1v_1^2}{r_1^3} - \frac{4c_3\left((c_2 + c_6)r_1 - 3c_3s_u\right)u_1^2v_1}{3r_1^4} \right] \\
&\quad \times \left(c_2u_1 + c_3v_1 + r_1\right) + \frac{1}{2!}\left[-\frac{2u_1}{r_1} + \frac{2c_3u_1v_1}{r_1^2} + \frac{2(c_2r_1 - 2c_3s_\mu)u_1^2}{3r_1^3} - \frac{2c_3^2u_1v_1^2}{r_1^3} \right. \\
&\quad \left. - \frac{4c_3\left((c_2 + c_6)r_1 - 3c_3s_\mu\right)u_1^2v_1}{3r_1^4} \right]^2 \times \left[c_1u_1 + c_2(c_2u_1 + c_3v_1 + r_1) + c_3\left(c_5u_1 + c_6v_1 + s_\mu\right) \right] \\
&\quad + \frac{1}{3!}\left[-\frac{2u_1}{r_1} + \frac{2c_3u_1v_1}{r_1^2} + \frac{2(c_2r_1 - 2c_3s_\mu)u_1^2}{3r_1^3} - \frac{2c_3^2u_1v_1^2}{r_1^3} - \frac{4c_3\left((c_2 + c_6)r_1 - 3c_3s_\mu\right)u_1^2v_1}{3r_1^4} \right]^3 \\
&\quad \times \left[(c_1c_2 + c_3c_4)u_1 + (c_1 + c_2^2 + c_3c_5)(c_2u_1 + c_3v_1 + r_1) + (c_2c_3 + c_3c_6)(c_5u_1 + c_6v_1 + s_\mu) \right] + \cdots
\end{aligned}$$

$$
\begin{aligned}
&= u_1 - \frac{2c_2}{r_1}u_1^2 + \frac{2c_2c_3}{r_1^2}u_1^2v_1 + \frac{2c_2\left(c_2r_1 - 2c_3s_\mu\right)}{3r_1^3}u_1^3 - \frac{2c_3}{r_1}u_1v_1 + \frac{2c_3^2}{r_1^2}u_1v_1^2 \\
&\quad + \frac{2c_3\left(c_2r_1 - 2c_3s_\mu\right)}{3r_1^3}u_1^2v_1 - \frac{2r_1}{r_1}u_1 + \frac{2c_3r_1}{r_1^2}u_1v_1 + \frac{2r_1\left(c_2r_1 - 2c_3s_\mu\right)}{3r_1^3}u_1^2 \\
&\quad - \frac{4c_3r_1\left(\left(c_2 + c_6\right)r_1 - 3c_3s_\mu\right)}{3r_1^4}u_1^2v_1 - \frac{2c_3^2r_1}{r_1^3}u_1v_1^2 + \frac{2c_1}{r_1^2}u_1^3 + \frac{2c_2^2}{r_1^2}u_1^3 \\
&\quad + \frac{2c_2c_3}{r_1^2}u_1^2v_1 + \frac{2c_2r_1}{r_1^2}u_1^2 + \frac{2c_3c_5}{r_1^2}u_1^3 + \frac{2c_3c_6}{r_1^2}u_1^2v_1 + \frac{2c_3s_\mu}{r_1^2}u_1^2 - \frac{4c_2c_3r_1}{r_1^3}u_1^2v_1 \\
&\quad - \frac{4c_3^2s_\mu}{r_1^3}u_1^2v_1 - \frac{4c_2r_1\left(c_2r_1 - 2c_3s_\mu\right)}{3r_1^4}u_1^3 - \frac{4c_3s_\mu\left(c_2r_1 - 2c_3s_\mu\right)}{3r_1^4}u_1^3 \\
&\quad - \frac{4u_1^3}{3r_1^3}\Big[\left(c_1 + c_2^2 + c_3c_5\right)r_1 + \left(c_2c_3 + c_3c_6\right)s_\mu\Big] + \cdots \\
&= -u_1 + \frac{2\left(c_2r_1 + c_3s_\mu\right)}{3r_1^2}u_1^2 - \frac{2c_3\left(c_2r_1 - c_6r_1 + 2c_3s_\mu\right)}{3r_1^3}u_1^2v_1 \\
&\quad - \frac{2\left[2c_3s_\mu r_1\left(c_2 + c_6\right) - r_1^2\left(c_1 + c_3c_5\right) - 4c_3^2s_\mu^2\right]}{3r_1^4}u_1^3 + \cdots
\end{aligned}
$$

Similarly,

$$
\begin{aligned}
\varphi_{12}^-\left(u_1, v_1\right) =& v_1 - \frac{2s_\mu}{r_1}u_1 - \frac{2\left(c_6r_1 - c_3s_\mu\right)}{r_1^2}u_1v_1 + \frac{2s_\mu\left(c_2r_1 + 3c_6r_1 - 2c_3s_\mu\right)}{3r_1^3}u_1^2 - \frac{2c_3\left(c_3s_\mu - c_6r_1\right)}{r_1^3}u_1v_1^2 \\
&+ \frac{2\xi_1}{3r_1^4}u_1^2v_1 - \frac{2\left[2c_3s_\mu r_1\left(c_2 + c_6\right) - r_1^2\left(c_1 + c_3c_5\right) - 4c_3^2s_\mu^2\right]}{3r_1^4}u_1^3 + \cdots,
\end{aligned}
$$

with $\xi_1 = c_6r_1^2\left(c_2 + 3c_6\right) - 2r_1c_3\left(c_2 + 5c_6\right)s_\mu + 6c_3^2s_\mu^2$.
We define the left-return map $\varphi^- : \left\{\bar{\Sigma} : u_1, v_1 < 0\right\} \mapsto \{\tilde{\Sigma} : \ u_2, v_2 > 0\}$ as

$$
\varphi^-\left(u_1, v_1, \mu\right) = \begin{pmatrix} \varphi_{11}^-\left(u_1, v_1, \mu\right) \\ \varphi_{12}^-\left(u_1, v_1, \mu\right) \end{pmatrix}.
$$

Using a similar approach, we can write (5.1b) as the system

$$
q_1 = q_2 + t_2N_2\left(t_2\right)\tilde{g}^+\left(q_2\right), \tag{5.8}
$$

the equation is equivalent to

$$
\begin{pmatrix} 0 \\ u_1 \\ v_1 \end{pmatrix} = \begin{pmatrix} 0 \\ u_2 \\ v_2 \end{pmatrix} + \begin{pmatrix} t_2e_1^TN_2\left(t_2\right)\tilde{g}\left(q_2\right) \\ t_2e_2^TN_2\left(t_2\right)\tilde{g}\left(q_2\right) \\ t_2e_3^TN_2\left(t_2\right)\tilde{g}\left(q_2\right) \end{pmatrix}, \tag{5.9}
$$

where

$$N_2(t_2) = I + \frac{t_2}{2!}\tilde{A}_2 + \frac{t_2^2}{3!}\tilde{A}_2^2 + \frac{t_2^3}{4!}\tilde{A}_2^3 + \cdots.$$

From the Eq (5.9), we could obtain

$$t_2 e_1^T N_2(t_2)\,\tilde{g}^+(q_2) = 0.$$

Upon observation, we note that the function

$$G_2(t_2, u_2, v_2) = e_1^T N_2(t_2)\,\tilde{g}^+(q_2) = v_2 + \frac{t_2}{2}\left(r_\mu + d_5 u_2 + d_6 v_2\right) + \frac{t_2^2}{6}\eta_2 + \cdots$$

where $\eta_2 = d_6 r_\mu + d_5 s_2 + (d_2 + d_6) d_5 u_2 + \left(d_4 + d_3 d_5 + d_6^2\right) v_2$, with $r_\mu = r_2 + \mu$ and $s_2 = \frac{r_1 r_2}{s_1}$, satisfies $G_2(0,0,0) = 0$ and $\frac{\partial G_2}{\partial t_2}(0,0,0) = \frac{r_\mu}{2} \neq 0$. Therefore, by the implicit function theorem(IFT), there exists a function related to $t_2(u_2, v_2)$ such that $G_2(t_2(u_2, v_2), u_2, v_2) \equiv 0$ in a neighborhood of $(0,0,0)$. This function is expressed as

$$t_2(u_2, v_2) = -\frac{2v_2}{r_\mu} + \frac{2d_5 u_2 v_2}{r_\mu^2} + \frac{2\left(d_6 r_\mu - 2d_5 s_2\right) v_2^2}{3r_\mu^3} - \frac{2d_5^2 u_2^2 v_2}{r_\mu^3} - \frac{4d_5\left((d_2 + d_6) r_\mu - 3d_5 s_2\right) u_2 v_2^2}{3r_\mu^4} + \cdots.$$

By substituting t_2 into the second and third equations of (5.9), we obtain

$$\begin{pmatrix} u_1 \\ v_1 \end{pmatrix} = \begin{pmatrix} \varphi_{21}^+(u_2, v_2) \\ \varphi_{22}^+(u_2, v_2) \end{pmatrix}, \tag{5.10}$$

where

$$\begin{aligned}
\varphi_{21}^+(u_2, v_2) =& u_2 - \frac{2s_2 v_2}{r_\mu} - \frac{2\left(d_2 r_\mu - d_5 s_2\right) u_2 v_2}{r_\mu^2} + \frac{2s_2\left((3d_2 + d_6) r_\mu - 2d_5 s_2\right) v_2^2}{3r_\mu^3} + \frac{2d_5\left(d_2 r_\mu - d_5 s_2\right) u_2^2 v_2}{r_\mu^3} \\
&+ \frac{2\xi_2 u_2 v_2^2}{3r_\mu^4} + \frac{2\left[r_\mu^2(d_2 d_3 - 2d_1) + 2d_2 s_2\left(2d_5 s_2 - d_6 r_\mu - d_2 r_\mu\right)\right]}{3r_\mu^4} v_2^3 + \cdots \\
\varphi_{22}^+(u_2, v_2) =& -v_2 + \frac{2\left(d_5 s_2 + d_6 r_\mu\right) v_2^2}{3r_\mu^2} + \frac{2d_5\left((d_2 - d_6) r_\mu - 2d_5 s_2\right) u_2 v_2^2}{3r_\mu^3} \\
&- \frac{2\left(2d_5 s_2 r_\mu (d_2 + d_6) - r_\mu^2(d_4 + d_3 d_5) - 4d_5^2 s_2^2\right) v_2^3}{3r_\mu^4} + \cdots
\end{aligned}$$

where $\xi_2 = 6d_5^2 s_2^2 - 2d_5 s_2 (5d_2 + d_6) r_\mu + d_2 (3d_2 + d_6) r_\mu^2$. We define the right-return map

$$\varphi^+ : \left\{\tilde{\Sigma} : u_2, v_2 > 0\right\} \mapsto \left\{\tilde{\Sigma} : u_1, v_1 < 0\right\}$$

as

$$\varphi^+(u_2, v_2, \mu) = \begin{pmatrix} \varphi_{21}^+(u_2, v_2, \mu) \\ \varphi_{22}^+(u_2, v_2, \mu) \end{pmatrix}.$$

The Poincaré map is defined as the composition of the half-return maps φ^- and φ^+. It maps the set $\Omega : \{\tilde{\Sigma} : u, v < 0\}$ to $\{\tilde{\Sigma} : u, v < 0\}$ given by

$$\Omega(u, v, \mu) = \varphi^+ \left(\varphi^-(u, v, \mu)\right) = \begin{pmatrix} \Omega_1(u, v, \mu) \\ \Omega_2(u, v, \mu) \end{pmatrix}, \tag{5.11}$$

where Ω_1 and Ω_2 are given as

$$\begin{aligned}
\Omega_1(u, v, u) = &\left(\frac{4s_2 s_\mu}{r_1 r_\mu} - 1\right)u - \frac{2s_2}{r_\mu}v + \left[\frac{4s_2\left(c_6 r_1 - c_3 s_\mu\right)}{r_1^2 r_\mu} + \frac{2\left(d_2 r_\mu - d_5 s_2\right)}{r_\mu^2}\right. \\
&\left. - \frac{8s_2 s_\mu\left(\left(3d_2 + d_6\right) r_\mu - 2d_5 s_2\right)}{3r_1 r_u^3}\right]uv + \left[\frac{2\left(c_2 r_1 + c_3 s_\mu\right)}{3r_1^2}\right. \\
&\left. - \frac{4s_2 s_\mu(c_2 r_1 + 3c_6 r_1 - 2c_3 s_\mu)}{3r_1^3 r_\mu} - \frac{4s_\mu\left(d_2 r_\mu - d_5 s_2\right)}{r_1 r_\mu^2}\right. \\
&\left. + \frac{8s_2 s_\mu^2\left(\left(3d_2 + d_6\right) r_\mu - 2d_5 s_2\right)}{3r_1^2 r_\mu^3}\right]u^2 + \frac{2s_2\left(\left(3d_2 + d_6\right) r_\mu - 2d_5 s_2\right)}{3r_\mu^3}v^2 + \cdots
\end{aligned}$$

$$\begin{aligned}
\Omega_2\left(u, v, \mu\right) = &\frac{2s_\mu}{r_1}u - v + \left[\frac{2\left(c_6 r_1 - c_3 s_\mu\right)}{r_1^2} - \frac{8s_\mu\left(d_5 s_2 + d_6 r_\mu\right)}{3r_1 r_\mu^2}\right]uv \\
&+ \left[\frac{8s_\mu^2\left(d_5 s_2 + d_6 r_\mu\right)}{3r_1^2 r_\mu^2} - \frac{2s_\mu\left(c_2 r_1 + 3c_6 r_1 - 2c_3 s_\mu\right)}{3r_1^3}\right]u^2 \\
&+ \frac{2\left(d_5 s_2 + d_6 r_\mu\right)}{3r_\mu^2}v^2 + \cdots.
\end{aligned}$$

Then, the fixed points (u, v) of this map are determined by

$$\begin{cases} \Omega_1(u, v, \mu) = u, \\ \Omega_2(u, v, \mu) = v. \end{cases} \tag{5.12}$$